

Bridging the Gap Between Adversarial Robustness and Optimization Bias

Fartash Faghri^{2,3*}Sven Gowal⁴Cristina Vasconcelos¹David J. Fleet^{1,2,3}Fabian Pedregosa¹Nicolas Le Roux^{1,5}¹Google Research ²University of Toronto ³Vector Institute ⁴DeepMind ⁵Mila

Abstract

We demonstrate that the choice of optimizer, neural network architecture, and regularizer significantly affect the adversarial robustness of linear neural networks, providing guarantees without the need for adversarial training. To this end, we revisit a known result linking maximally robust classifiers and minimum norm solutions, and combine it with recent results on the implicit bias of optimizers. First, we show that, under certain conditions, it is possible to achieve both perfect standard accuracy and a certain degree of robustness, simply by training an overparametrized model using the implicit bias of the optimization. In that regime, there is a direct relationship between the type of the optimizer and the attack to which the model is robust. To the best of our knowledge, this work is the first to study the impact of optimization methods such as sign gradient descent and proximal methods on adversarial robustness. Second, we characterize the robustness of linear convolutional models, showing that they resist attacks subject to a constraint on the Fourier- ℓ_∞ norm. To illustrate these findings we design a novel Fourier- ℓ_∞ attack that finds adversarial examples with controllable frequencies. We evaluate Fourier- ℓ_∞ robustness of adversarially-trained deep CIFAR-10 models from the standard RobustBench benchmark and visualize adversarial perturbations.

1 Introduction

Deep neural networks achieve high accuracy on standard test sets, yet Szegedy et al. [1] showed that any natural input correctly classified by a neural network can be modified with adversarial perturbations that fool the network into misclassification, even when such perturbations are constrained to be small enough that do not significantly affect human perception. Adversarial training improves model robustness through training on adversarial samples [2] and can be interpreted as approximately solving a saddle-point problem [3]. Adversarial training is the state-of-the-art approach to adversarial robustness [4, 5] and alternative approaches are more likely to exhibit spurious robustness [6]. Nevertheless, adversarial training is computationally expensive compared to standard training, as it involves an alternated optimization. Adversarial training also exhibits a trade-off between standard generalization and adversarial robustness. That is, it achieves improved *robust accuracy*, on adversarially perturbed data, at the expense of *standard accuracy*, the probability of correct predictions on natural data [7]. This adversarial robustness trade-off has been shown to be intrinsic in a number of toy examples [8], independent of the learning algorithm in some cases [9]. Alternatives to adversarial training have been proposed to reduce this trade-off, but a gap remains in practice [10].

*Work done during an internship at Google Research. Code available at: https://github.com/fartashf/robust_bias. Correspondence to: Fartash Faghri <faghri@cs.toronto.edu>.

Here we consider connections between the adversarial robustness trade-off and optimization biases in training overparametrized models. Deep learning models can often achieve interpolation, i.e., they have the capacity to exactly fit the training data [11]. Their ability to generalize well in such cases has been attributed to an implicit bias toward simple solutions [12, 13].

Our main contribution is to connect two large bodies of work on adversarial robustness and optimization bias. Focusing on models that achieve interpolation, we use the formulation of a *Maximally Robust Classifier* from robust optimization [14]. We theoretically demonstrate that the choice of optimizer (Corollary 1), neural network architecture (Corollary 2), and regularizer (Corollary 3), significantly affect the adversarial robustness of linear neural networks. Even for linear models, the impact of these choices had not been characterized precisely prior to our work. We observe that, in contrast to adversarial training, under certain conditions we can find maximally robust classifiers at no additional computational cost.

Based on our theoretical results on the robustness of linear convolutional models to Fourier attacks, we introduce a new class of attacks in the Fourier domain. In particular, we design the Fourier- ℓ_∞ attack and illustrate our theoretical results. Extending to non-linear models, we attack adversarially-trained deep models on CIFAR-10 from RobustBench benchmark [5] and find low and high frequency adversarial perturbations by directly controlling spectral properties through Fourier constraints. This example demonstrates how understanding maximal robustness of linear models is a stepping stone to understanding and guaranteeing robustness of non-linear models.

2 No Trade-offs with Maximally Robust Classifiers

We start by defining adversarial robustness and the robustness trade-off in adversarial training. Then, Section 2.1 provides an alternative formulation to adversarial robustness that avoids the robustness trade-off. Let $\mathcal{D} = \{(\mathbf{x}_i, y_i)\}_{i=1}^n$ denote a training set sampled I.I.D. from a distribution, where $\mathbf{x}_i \in \mathbb{R}^d$ are features and $y_i \in \{-1, +1\}$ are binary labels. A binary classifier is a function $\varphi : \mathbb{R}^d \rightarrow \mathbb{R}$, and its prediction on an input \mathbf{x} is given by $\text{sign}(\varphi(\mathbf{x})) \in \{-1, +1\}$. The aim in supervised learning is to find a classifier that accurately classifies the training data and generalizes to unseen test data. One standard framework for training a classifier is Empirical Risk Minimization (ERM), $\arg \min_{\varphi \in \Phi} \mathcal{L}(\varphi)$, where $\mathcal{L}(\varphi) := \mathbb{E}_{(\mathbf{x}, y) \sim \mathcal{D}} \zeta(y\varphi(\mathbf{x}))$, Φ is a family of classifiers, and $\zeta : \mathbb{R} \rightarrow \mathbb{R}^+$ is a loss function that we assume to be strictly monotonically decreasing to 0, i.e., $\zeta' < 0$. Examples are the exponential loss, $\exp(-\hat{y}y)$, and the logistic loss, $\log(1 + \exp(-\hat{y}y))$.

Given a classifier, an adversarial perturbation $\delta \in \mathbb{R}^d$ is any small perturbation that changes the model prediction, i.e., $\text{sign}(\varphi(\mathbf{x} + \delta)) \neq \text{sign}(\varphi(\mathbf{x}))$, $\|\delta\| \leq \varepsilon$, where $\|\cdot\|$ is a norm on \mathbb{R}^d , and ε is an arbitrarily chosen constant. It is common to use norm-ball constraints to ensure perturbations are small (e.g., imperceptible in images) but other constraints exist [15]. Commonly used are the ℓ_p norms,

$\|\mathbf{v}\|_p = \left(\sum_{i=0}^{d-1} [v]_i^p\right)^{1/p}$, where $[v]_i$ denotes the i -th element of a vector \mathbf{v} , for $i = 0, \dots, d-1$.

In practice, an adversarial perturbation, δ , is found as an approximate solution to the following optimization problem,

$$\max_{\delta: \|\delta\| \leq \varepsilon} \zeta(y\varphi(\mathbf{x} + \delta)). \quad (1)$$

Under certain conditions, closed form solutions exist to the optimization problem in (1). For example, Goodfellow et al. [2] observed that the maximal ℓ_∞ -bounded adversarial perturbation against a linear model (i.e. one causing the maximum change in the output) is the sign gradient direction scaled by ε .

Madry et al. [3] defined an adversarially robust classifier as the solution to the saddle-point optimization problem,

$$\arg \min_{\varphi \in \Phi} \mathbb{E}_{(\mathbf{x}, y) \sim \mathcal{D}} \max_{\delta: \|\delta\| \leq \varepsilon} \zeta(y\varphi(\mathbf{x} + \delta)). \quad (2)$$

The saddle-point adversarial robustness problem is the robust counter-part to empirical risk minimization where the expected loss is minimized on worst-case adversarial samples defined as solutions to (1). Adversarial Training [2] refers to solving (2) using an alternated optimization. It is computationally expensive because it often requires solving (1) many times.

The main drawback of defining the adversarially robust classifier using (2), and a drawback of adversarial training, is that the parameter ε needs to be known or tuned. The choice of ε controls a trade-off between standard accuracy on samples of the dataset \mathcal{D} versus the robust accuracy, i.e., the accuracy on adversarial samples. At one extreme $\varepsilon = 0$, where (2) reduces to ERM. At the other, as

$\varepsilon \rightarrow \infty$, all inputs in \mathbb{R}^d are within the ε -ball of every training point and can be an adversarial input. The value of the inner max in (2) for a training point \mathbf{x}, y is the loss of the most confident prediction over \mathbb{R}^d that is predicted as $-y$. For large enough ε , the solution to (2) is a classifier predicting the most frequent label, i.e., $\varphi(\cdot) = p^*$, where p^* is the solution to $\arg \min_p n_{-1}\zeta(-p) + n_{+1}\zeta(p)$, and n_{-1}, n_{+1} are the number of negative and positive training labels.

Robust accuracy is often a complementary generalization metric to standard test accuracy. In practice, we prefer a classifier that is accurate on the test set, and that additionally, achieves maximal robustness. The saddle-point formulation makes this challenging without the knowledge of the maximal ε . This trade-off has been studied in various works [7, 10, 16, 8, 9]. Regardless of the trade-off imposed by ε , adversarial training is considered to be the state-of-the-art for adversarial robustness. The evaluation is based on the robust accuracy achieved at fixed ε 's even though the standard accuracy is usually lower than a comparable non-robust model [5, 4].

2.1 Maximally Robust Classifier

In order to avoid the trade-off imposed by ε in adversarial robustness, we revisit a definition from robust optimization.

Definition 2.1. A **Maximally Robust Classifier** (Ben-Tal et al. [14]) is a solution to

$$\arg \max_{\varphi \in \Phi} \{ \varepsilon \mid y_i \varphi(\mathbf{x}_i + \boldsymbol{\delta}) > 0, \forall i, \|\boldsymbol{\delta}\| \leq \varepsilon \}. \quad (3)$$

Compared with the saddle-point formulation (2), ε in (3) is not an arbitrary constant. Rather, it is maximized as part of the optimization problem. Moreover, the maximal ε in this definition does not depend on a particular loss function. Note, a maximally robust classifier is not necessarily unique.

The downside of (3) is that the formulation requires the training data to be separable so that (3) is non-empty, i.e. there exists $\varphi \in \Phi$ such that $\forall i, y_i \varphi(\mathbf{x}_i) > 0$. In most deep learning settings, this is not a concern as models are large enough that they can interpolate the training data, i.e. for any dataset there exists φ such that $\varphi(\mathbf{x}_i) = y_i$. An alternative formulation is to modify the saddle-point problem and include an outer maximization on ε by allowing a non-zero slack loss. However, the new slack loss reimposes a trade-off between standard and robust accuracy (See Appendix A).

One can also show that adversarial training, i.e., solving the saddle-point problem (2), does not necessarily find a maximally robust classifier. To see this, suppose we are given the maximal ε in (3). Further assume the minimum of (2) is non-zero. Then the cost in the saddle-point problem does not distinguish between the following two models: 1) a model that makes no misclassification errors but has low confidence, i.e. $\forall i, 0 < \max_{\boldsymbol{\delta}} y_i \varphi(\mathbf{x}_i + \boldsymbol{\delta}) \leq c_1$ for some small c_1 2) a model that classifies a training point, \mathbf{x}_j , incorrectly but is highly confident on all other training data and adversarially perturbed ones, i.e. $\forall i \neq j, 0 < c_2 < \max_{\boldsymbol{\delta}} y_i \varphi(\mathbf{x}_i + \boldsymbol{\delta})$. The second model can incur a loss $n\zeta(c_1) - (n-1)\zeta(c_2)$ on \mathbf{x}_j while being no worse than the first model according to the cost of the saddle-point problem. The reason is another trade-off between standard and robust accuracy caused by taking the expectation over data points.

2.2 Linear Models: Maximally Robust is the Minimum Norm Classifier

Given a dataset and a norm, what is the maximally robust linear classifier with respect to that norm? In this section, we revisit a result from Ben-Tal et al. [14] for classification.

Definition 2.2 (Dual norm). Let $\|\cdot\|$ be a norm on \mathbb{R}^n . The associated *dual norm*, denoted $\|\cdot\|_*$, is defined as $\|\boldsymbol{\delta}\|_* = \sup_{\mathbf{x}} \{ |\langle \boldsymbol{\delta}, \mathbf{x} \rangle| \mid \|\mathbf{x}\| \leq 1 \}$.

Definition 2.3 (Linear Separability). We say a dataset is linearly separable if there exists \mathbf{w}, b such that $y_i(\mathbf{w}^\top \mathbf{x}_i + b) > 0$ for all i .

Lemma 2.1 (Maximally Robust Linear Classifier (Ben-Tal et al. [14], §12)). *For linear models and linearly separable data, the following problems are equivalent; i.e., from a solution of one, a solution of the other is readily found.*

$$\text{Maximally robust classifier: } \arg \max_{\mathbf{w}, b} \{ \varepsilon \mid y_i(\mathbf{w}^\top (\mathbf{x}_i + \boldsymbol{\delta}) + b) > 0, \forall i, \|\boldsymbol{\delta}\| \leq \varepsilon \}, \quad (4)$$

$$\text{Maximum margin classifier: } \arg \max_{\mathbf{w}, b: \|\mathbf{w}\|_* \leq 1} \{ \varepsilon \mid y_i(\mathbf{w}^\top \mathbf{x}_i + b) \geq \varepsilon, \forall i \}, \quad (5)$$

$$\text{Minimum norm classifier: } \arg \min_{\mathbf{w}, b} \{ \|\mathbf{w}\|_* \mid y_i(\mathbf{w}^\top \mathbf{x}_i + b) \geq 1, \forall i \}. \quad (6)$$

The expression $\min_i y_i(\mathbf{w}^\top \mathbf{x}_i + b)/\|\mathbf{w}\|$ is the margin of a classifier \mathbf{w} that is the distance of the nearest training point to the classification boundary, i.e. the line $\{\mathbf{v} : \mathbf{w}^\top \mathbf{v} = -b\}$.

We provide a proof for general norms based on Ben-Tal et al. [14] in [Appendix B.1](#). Each formulation in [Lemma 2.1](#) is connected to a wide array of results that can be transferred to other formulations. Maximally robust classification is one example of a problem in robust optimization that can be reduced and solved efficiently. Other problems such as robust regression as well as robustness to correlated input perturbations have been studied prior to deep learning [14].

On the other hand, maximum margin and minimum norm classification have long been popular because of their generalization guarantees. Recent theories for overparametrized models link the margin and the norm of a model to generalization [13]. Although the tools are different, connecting the margin and the norm of a model has also been the basis of generalization theories for Support Vector Machines and AdaBoost [17, 18]. Maximum margin classification does not require linear separability, because there can exist a classifier with $\varepsilon < 0$ that satisfies the margin constraints. Minimum norm classification is the easiest formulation to work with in practice as it does not rely on ε nor δ and minimizes a function of the weights subject to a set of constraints.

In what follows, we use [Lemma 2.1](#) to transfer recent results about minimum norm classification to maximally robust classification. These results have been the basis for explaining generalization properties of deep learning models [13, 19].

3 Implicit Robustness of Optimizers

The most common approach to empirical risk minimization (ERM) is through gradient-based optimization. As we will review shortly, Gunasekar et al. [12] showed that gradient descent, and more generally steepest descent methods, have an implicit bias towards minimum norm solutions. From the infinitely many solutions that minimize the empirical risk, we can characterize the one found by steepest descent. Using [Lemma 2.1](#), we show that such a classifier is also maximally robust w.r.t. a specific norm.

Recall that ERM is defined as $\arg \min_{\varphi \in \Phi} \mathcal{L}(\varphi)$, where $\mathcal{L}(\varphi) = \mathbb{E}_{(x,y) \sim \mathcal{D}} \zeta(y\varphi(x))$. Here we assume \mathcal{D} is a finite dataset of size n . For the linear family of functions, we write $\mathcal{L}(\mathbf{w}, b)$. Hereafter, we rewrite the loss as $\mathcal{L}(\mathbf{w})$ and use an augmented representation with a constant 1 dimension. For linearly separable data and overparametrized models ($d > n$), there exist infinitely many linear classifiers that minimize the empirical risk [12]. We will find it convenient to ignore the scaling and focus on the normalized vector $\mathbf{w}/\|\mathbf{w}\|$, i.e. the direction of \mathbf{w} . We will say that the sequence $\mathbf{w}_1, \mathbf{w}_2, \dots$ converges in direction to a vector \mathbf{v} if $\lim_{t \rightarrow \infty} \mathbf{w}_t/\|\mathbf{w}_t\| = \mathbf{v}$.

3.1 Steepest Descent on Fully-Connected Networks

Definition 3.1 (Steepest Descent). Let $\|\cdot\|$ denote a norm, f a function to be minimized, and γ a step size. The steepest descent method associated with this norm finds

$$\mathbf{w}_{t+1} = \mathbf{w}_t + \gamma \Delta \mathbf{w}_t, \quad \text{where } \Delta \mathbf{w}_t \in \arg \min_{\mathbf{v}} \langle \nabla f(\mathbf{w}_t), \mathbf{v} \rangle + \frac{1}{2} \|\mathbf{v}\|^2. \quad (7)$$

The steepest descent step, $\Delta \mathbf{w}_t$, can be equivalently written as $-\|\nabla f(\mathbf{w}_t)\|_* g_{\text{nst}}$, where $g_{\text{nst}} \in \arg \min \{\langle \nabla f(\mathbf{w}_t), \mathbf{v} \rangle \mid \|\mathbf{v}\| = 1\}$. A proof can be found in [20, §9.4].

Remark. For some p -norms, steepest descent steps have closed form expressions. Gradient Descent (GD) is steepest descent w.r.t. ℓ_2 norm where $-\nabla f(\mathbf{w}_t)$ is a steepest descent step. Sign gradient descent is steepest descent w.r.t. ℓ_∞ norm where $-\|\nabla f(\mathbf{w}_t)\|_1 \text{sign}(\nabla f(\mathbf{w}_t))$ is a steepest descent step. Coordinate Descent (CD) is steepest descent w.r.t. ℓ_1 norm where $-\nabla f(\mathbf{w}_t)_i \mathbf{e}_i$ is a steepest descent step (i is the coordinate for which the gradient has the largest absolute magnitude).

Theorem 3.1 (Implicit Bias of Steepest Descent (Gunasekar et al. [12] (Theorem 5))). *For any separable dataset $\{\mathbf{x}_i, y_i\}$ and any norm $\|\cdot\|$, consider the steepest descent updates from (7) for minimizing the empirical risk $\mathcal{L}(\mathbf{w})$ (defined in [Section 2](#)) with the exponential loss, $\zeta(z) = \exp(-z)$. For all initializations \mathbf{w}_0 , and all bounded step-sizes satisfying a known upper bound, the iterates \mathbf{w}_t satisfy*

$$\lim_{t \rightarrow \infty} \min_i \frac{y_i \mathbf{w}_t^\top \mathbf{x}_i}{\|\mathbf{w}_t\|} = \max_{\mathbf{w} : \|\mathbf{w}\| \leq 1} \min_i y_i \mathbf{w}^\top \mathbf{x}_i. \quad (8)$$

In particular, if a unique maximum margin classifier $\mathbf{w}_{\|\cdot\|}^* = \arg \max_{\mathbf{w}: \|\mathbf{w}\| \leq 1} \min_i y_i \mathbf{w}^\top \mathbf{x}_i$ exists, the limit direction converges to it, i.e. $\lim_{t \rightarrow \infty} \frac{\mathbf{w}_t}{\|\mathbf{w}_t\|} = \mathbf{w}_{\|\cdot\|}^*$.

In other words, the margin converges to the maximum margin and if the maximum margin classifier is unique, the iterates converge in direction to $\mathbf{w}_{\|\cdot\|}^*$. We use this result to derive our [Corollary 1](#).

Corollary 1 (Implicit Robustness of Steepest Descent). *For any linearly separable dataset and any norm $\|\cdot\|$, steepest descent iterates minimizing the empirical risk, $\mathcal{L}(\mathbf{w})$, satisfying the conditions of [Theorem 3.1](#), converge in direction to a maximally robust classifier,*

$$\arg \max_{\mathbf{w}} \{ \varepsilon \mid y_i \mathbf{w}^\top (\mathbf{x}_i + \boldsymbol{\delta}) > 0, \forall i, \|\boldsymbol{\delta}\|_* \leq \varepsilon \}.$$

In particular, a maximally robust classifier against ℓ_1 , ℓ_2 , and ℓ_∞ is reached, respectively, by sign gradient descent, gradient descent, and coordinate descent.

Proof. By [Theorem 3.1](#), the margin of the steepest descent iterates, $\min_i \frac{y_i \mathbf{w}_t^\top \mathbf{x}_i}{\|\mathbf{w}_t\|}$, converges as $t \rightarrow \infty$ to the maximum margin, $\max_{\mathbf{w}: \|\mathbf{w}\| \leq 1} \min_i y_i \mathbf{w}^\top \mathbf{x}_i$. By [Lemma 2.1](#), any maximum margin classifier w.r.t. $\|\cdot\|$ gives a maximally robust classifier w.r.t. $\|\cdot\|_*$. \square

[Corollary 1](#) implies that for overparametrized linear models, we obtain guaranteed robustness by an appropriate choice of optimizer without the additional cost and trade-off of adversarial training. We note that [Theorem 3.1](#) and [Corollary 1](#), characterize linear models, but do not account for the bias b . We can close the gap with an augmented input representation, to include the bias explicitly. Or one could preprocess the data, removing the mean before training.

To extend [Corollary 1](#) to deep learning models one can use generalizations of [Theorem 3.1](#). For the special case of gradient descent, [Theorem 3.1](#) has been generalized to multi-layer fully-connected linear networks and a larger family of strictly monotonically decreasing loss functions including the logistic loss [[21](#), [Theorem 2](#)].

3.2 Gradient Descent on Linear Convolutional Networks

In this section, we show that even for linear models, the choice of the architecture affects implicit robustness, which gives another alternative for achieving maximal robustness. We use a generalization of [Theorem 3.1](#) to linear convolutional models.

Definition 3.2 (Linear convolutional network). An L -layer convolutional network with 1-D circular convolution is parameterized using weights of $L - 1$ convolution layers, $\mathbf{w}_1, \dots, \mathbf{w}_{L-1} \in \mathbb{R}^d$, and weights of a final linear layer, $\mathbf{w}_L \in \mathbb{R}^d$, such that the linear mapping of the network is

$$\varphi_{\text{conv}}(\mathbf{x}; \mathbf{w}_1, \dots, \mathbf{w}_L) := \mathbf{w}_L^\top (\mathbf{w}_{L-1} \star \dots (\mathbf{w}_1 \star \mathbf{x})).$$

Here, circular convolution is defined as $[\mathbf{w} \star \mathbf{x}]_i := \frac{1}{\sqrt{d}} \sum_{k=0}^{d-1} [\mathbf{w}]_{\overline{-k}} [\mathbf{x}]_{\overline{i+k}}$, where $[v]_i$ denotes the i -th element of a vector \mathbf{v} for $i = 0, \dots, d - 1$, and $\overline{i} = i \bmod d$.²

A linear convolutional network is equivalent to a linear model with weights $\mathbf{w} = \mathbf{w}_L \star (\dots \star (\mathbf{w}_2 \star \mathbf{w}_1))$ because of the associative property of convolution. In particular, for two-layer linear convolutional networks $\mathbf{w} = \mathbf{w}_2 \star \mathbf{w}_1$.

Definition 3.3 (Discrete Fourier Transform). $\mathcal{F}(\mathbf{w}) \in \mathbb{C}^d$ denotes the Fourier coefficients of \mathbf{w} where $[\mathcal{F}(\mathbf{w})]_d = \frac{1}{\sqrt{d}} \sum_{k=0}^{d-1} [\mathbf{w}]_k \exp(-\frac{2\pi j}{d} kd)$ and $j^2 = -1$.

Theorem 3.2 (Implicit Bias towards Fourier Sparsity ([Gunasekar et al. \[22\]](#), [Theorem 2, 2.a](#))). *Consider the family of L -layer linear convolutional networks and the sequence of gradient descent iterates, \mathbf{w}_t , minimizing the empirical risk, $\mathcal{L}(\mathbf{w})$, with the exponential loss, $\exp(-z)$. For almost all linearly separable datasets under known conditions on the step size and convergence of iterates, \mathbf{w}_t converges in direction to the classifier minimizing the norm of the Fourier coefficients given by*

$$\arg \min_{\mathbf{w}_1, \dots, \mathbf{w}_L} \{ \|\mathcal{F}(\mathbf{w})\|_{2/L} \mid y_i \langle \mathbf{w}, \mathbf{x}_i \rangle \geq 1, \forall i \}. \quad (9)$$

In particular, for two-layer linear convolutional networks the implicit bias is towards the solution with minimum ℓ_1 norm of the Fourier coefficients, $\|\mathcal{F}(\mathbf{w})\|_1$. For $L > 2$, the convergence is to a first-order stationary point.

²We use the usual definition of circular convolution in signal processing, rather than cross-correlation, $\mathbf{w}^\dagger \star \mathbf{x}$ with $[\mathbf{w}^\dagger]_i = [\mathbf{w}]_{\overline{-i}}$, which is used in deep learning literature, but not associative.

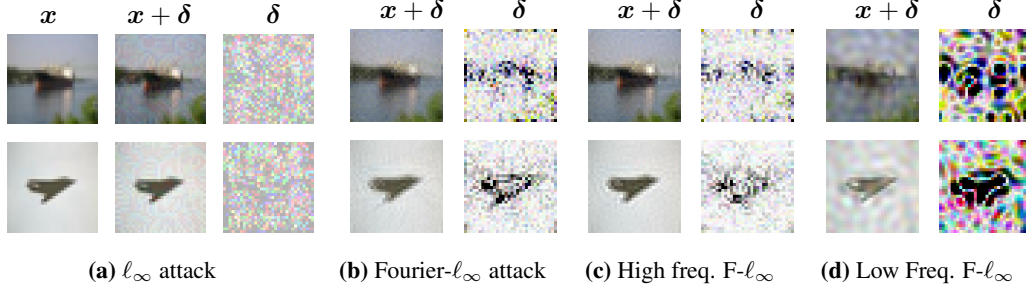


Figure 1: Adversarial attacks (ℓ_∞ and Fourier- ℓ_∞) against CIFAR-10 classification models. Fourier- ℓ_∞ perturbations (b) in the spatial domain are concentrated around subtle details of the object (darker means stronger perturbation). In contrast, ℓ_∞ perturbations (a) are perceived by people as random noise. Fourier- ℓ_∞ can also be controlled to be high or low frequency (c, d). It is more difficult to attack a standard model with only low frequency perturbations (for all attacks $\varepsilon = 8/255$ but for low frequency Fourier- ℓ_∞ $\varepsilon = 50/255$, otherwise attack fails). Appendix E.4 shows visualizations for variety of models in RobustBench.

We use this result to derive our Corollary 2.

Corollary 2 (Maximally Robust to Perturbations with Bounded Fourier Coefficients). *Consider the family of two-layer linear convolutional networks and the gradient descent iterates, w_t , minimizing the empirical risk. For almost all linearly separable datasets under conditions of Theorem 3.2, w_t converges in direction to a maximally robust classifier;*

$$\arg \max_{w_1, \dots, w_L} \{ \varepsilon \mid y_i \varphi_{\text{conv}}(x_i + \delta; \{w_l\}_{l=1}^L) > 0, \forall i, \|\mathcal{F}(\delta)\|_\infty \leq \varepsilon \}.$$

Proof in Appendix B.2. Corollary 2 implies that, at no additional cost, linear convolutional models are already maximally robust, but w.r.t. perturbations in the Fourier domain. We call attacks with ℓ_p constraints in the Fourier domain *Fourier- ℓ_p* attacks. Appendix F depicts various norm-balls in 3D to illustrate the significant geometrical difference between the Fourier- ℓ_∞ and other commonly used norm-balls for adversarial robustness. One way to understand Corollary 2 is to think of perturbations that succeed in fooling a linear convolutional network. Any such adversarial perturbation must have at least one frequency beyond the maximal robustness of the model. This condition is satisfied for perturbations with small ℓ_1 norm in the spatial domain, i.e., only a few pixels are perturbed.

3.3 Fourier Attacks

The predominant motivation for designing new attacks is to *fool* existing models. In contrast, our results characterize the attacks that existing models *perform best* against, as measured by maximal robustness. Based on Corollary 2 we design the Fourier- ℓ_p attack to verify our results. Some adversarial attacks exist with Fourier constraints [23, 24]. Sharma et al. [25] proposed a Fourier- ℓ_p attack that includes Fourier constraints in addition to ℓ_p constraints in the spatial domain. Our theoretical results suggest a more general class of attacks with only Fourier constraints.

The maximal ℓ_p -bounded adversarial perturbation against a linear model in (1) consists of real-valued constraints with a closed form solution. In contrast, maximal Fourier- ℓ_p has complex-valued constraints. In Appendix C we derive the Fourier- ℓ_∞ attack in closed form for linear models and provide the pseudo-code in Algorithm 1. To find perturbations as close as possible to natural corruptions such as blur, ε can be a matrix of constraints that is multiplied elementwise by δ . As our visualizations in Fig. 1 show, adversarial perturbations under bounded Fourier- ℓ_∞ can be controlled to be high frequency and concentrated on subtle details of the image, or low frequency and global. We observe that high frequency Fourier- ℓ_∞ attacks succeed more easily with smaller perturbations compared with low frequency attacks. The relative success of our band-limited Fourier attacks matches the empirical observation that the amplitude spectra of common ℓ_p attacks are largely band-limited as such attacks succeed more easily [26].

Algorithm 1 Fourier- ℓ_∞ Attack (see Appendix C)

Input: data x , label y , loss function ζ , classifier φ , perturbation size ε , number of attack steps m , dimensions d , Fourier transform \mathcal{F}

for $k = 1$ **to** m **do**

$\hat{g} = \mathcal{F}(\nabla_x \zeta(y\varphi(x)))$

$[\delta]_i = \varepsilon \frac{[\hat{g}]_i}{|[\hat{g}]_i|}, \forall i \in \{0, \dots, d-1\}$

$x = x + \mathcal{F}^{-1}(\delta)$

end for

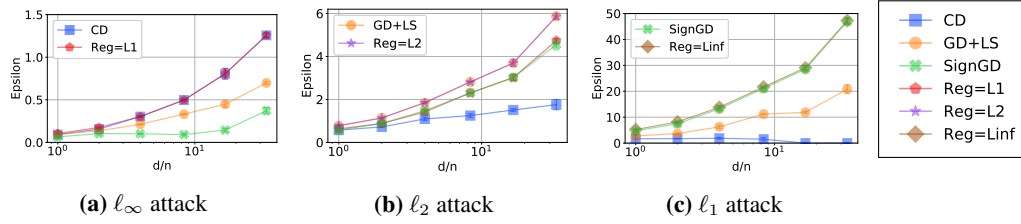


Figure 2: Maximally robust perturbation size (ε) for linear models against ℓ_∞ , ℓ_2 , and ℓ_1 attacks. For each attack, there exists one optimizer and one regularization method that finds a maximally robust classifier (inner legends). We compare Coordinate Descent (CD), Gradient Descent with Line Search (GD+LS), Sign Gradient Descent (SignGD), and explicit ℓ_1 , ℓ_2 , and ℓ_∞ regularization. The gap between methods grows with the overparametrization ratio (d/n). (More figures in [Appendix E.3](#))

4 Explicit Regularization

Above we discussed the impact of optimization method and model architecture on robustness. Here, we discuss explicit regularization as another choice that affects robustness.

Definition 4.1 (Regularized Classification). The regularized empirical risk minimization problem for linear classification is defined as $\hat{\mathbf{w}}(\lambda) = \arg \min_{\mathbf{w}} \mathbb{E}_{(\mathbf{x}, y) \sim \mathcal{D}} \zeta(y \mathbf{w}^\top \mathbf{x}) + \lambda \|\mathbf{w}\|$, where λ denotes a regularization constant, ζ is a monotone loss function, and \mathcal{D} is a dataset. For simplicity we assume this problem has a unique solution while the original ERM can have multiple solutions.

Theorem 4.1 (Maximum Margin Classifier using Regularization (Rosset et al. [27], Theorem 2.1)). Consider linearly separable datasets and monotonically non-increasing loss functions. Then as $\lambda \rightarrow 0$, the sequence of solutions, $\hat{\mathbf{w}}(\lambda)$, to the regularized problem in [Definition 4.1](#), converges in direction to a maximum margin classifier as defined in (5). Moreover, if the maximum margin classifier is unique,

$$\lim_{\lambda \rightarrow 0} \frac{\hat{\mathbf{w}}(\lambda)}{\|\hat{\mathbf{w}}(\lambda)\|} = \arg \max_{\mathbf{w}: \|\mathbf{w}\| \leq 1} \min_i y_i \mathbf{w}^\top \mathbf{x}_i. \quad (10)$$

The original proof in [27] was given specifically for ℓ_p norms, however we observe that their proof only requires convexity of the norm, so we state it more generally. Quasi-norms such as ℓ_p for $p < 1$ are not covered by this theorem. In addition, the condition on the loss function is weaker than our strict monotonic decreasing condition as shown in [21, Appendix A].

We use this result to derive our [Corollary 3](#).

Corollary 3 (Maximally Robust Classifier via Infinitesimal Regularization). For linearly separable data, under conditions of [Theorem 4.1](#), the sequence of solutions to regularized classification problems converges in direction to a maximally robust classifier. That is, $\lim_{\lambda \rightarrow 0} \hat{\mathbf{w}}(\lambda) / \|\hat{\mathbf{w}}(\lambda)\|$ converges to a solution of $\arg \max_{\mathbf{w}} \{\varepsilon \mid y_i \mathbf{w}^\top (\mathbf{x}_i + \boldsymbol{\delta}) > 0, \forall i, \|\boldsymbol{\delta}\|_* \leq \varepsilon\}$.

Proof. By [Theorem 4.1](#), the margin of the sequence of regularized classifiers, $\min_i y_i \frac{\hat{\mathbf{w}}(\lambda)^\top \mathbf{x}_i}{\|\hat{\mathbf{w}}(\lambda)\|}$, converges to the maximum margin, $\max_{\mathbf{w}: \|\mathbf{w}\| \leq 1} \min_i y_i \mathbf{w}^\top \mathbf{x}_i$. By [Lemma 2.1](#), any maximum margin classifier w.r.t. $\|\cdot\|$ gives a maximally robust classifier w.r.t. $\|\cdot\|_*$. \square

Assuming the solution to the regularized problem is unique, the regularization term replaces other implicit biases in minimizing the empirical risk. The regularization coefficient controls the trade-off between robustness and standard accuracy. The advantage of this formulation compared with adversarial training is that we do not need the knowledge of the maximally robust ε to find a maximally robust classifier. It suffices to choose an infinitesimal regularization coefficient. Wei et al. [28, Theorem 4.1] generalized [Theorem 4.1](#) for a family of classifiers that includes fully-connected networks with ReLU non-linearities, which allows for potential extension of [Corollary 3](#) to non-linear models. There remain gaps in this extension (see [Appendix D](#)).

Explicit regularization has been explored as an alternative approach to adversarial training [29, 30, 10, 31, 32]. To be clear, we do not propose a new regularization method but rather, we provide a framework for deriving and guaranteeing the robustness of existing and future regularization methods.

5 Experiments

This section empirically compares approaches to finding maximally robust classifiers. [Section 5.3](#) evaluates the robustness of CIFAR-10 [33] image classifiers against our Fourier- ℓ_∞ attack. We implement our attack in AutoAttack [34] and evaluate the robustness of recent defenses available in RobustBench [5]. Details of the experiments and additional visualizations are in [Appendix E](#).

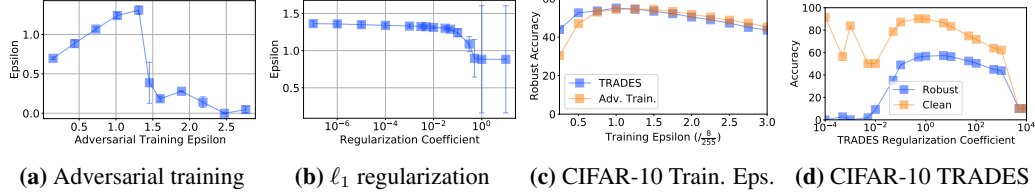


Figure 4: Trade-off in robustness against ℓ_∞ attack in linear models and CIFAR-10. We plot the maximally robust ε for adversarial training and explicit regularization. Robustness is controlled using ε in adversarial training (a) and regularization coefficient in explicit regularization (b). Using adversarial training we have to search for the maximal ε but for explicit regularization it suffices to choose a small regularization coefficient. Similarly, on CIFAR-10, the highest robustness at a fixed test ε is achieved for ε used during training (c). In contrast to optimal linear regularizations, TRADES shows degradation as the regularization coefficient decreases (d). Discussion in Section 5.2

5.1 Maximally Robust to ℓ_∞ , ℓ_2 , ℓ_1 , and Fourier- ℓ_∞ Bounded Attacks

Figs. 2 and 3 plot the maximally robust ε as a function of the overparametrization ratio d/n , where d is the model dimension and n is the number of data points. Fig. 2 shows robustness against ℓ_∞ , ℓ_2 , and ℓ_1 attacks for linear models. Coordinate descent and explicit ℓ_1 regularization find a maximally robust ℓ_∞ classifier. Coordinate descent and ℓ_2 regularization find a maximally robust ℓ_2 classifier. Sign gradient descent and ℓ_∞ regularization find a maximally robust ℓ_1 classifier. The gap between margins grows as d/n increases. Fig. 3 shows robustness against Fourier- ℓ_∞ attack; training a 2-layer linear convnet with gradient descent converges to a maximally robust classifier, albeit slowly.

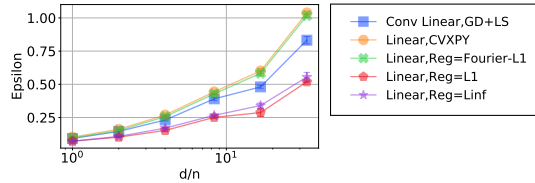


Figure 3: Maximally robust ε against Fourier- ℓ_∞ attack. Explicit Fourier- ℓ_1 regularization finds a maximally robust classifier as it achieves similar robustness as CVXPY’s solution. A linear convolutional model converges to a solution more slowly.

For these plots we synthesized linearly separable data focusing on overparametrized classification problems (i.e., $d > n$). Plotting the overparametrization ratio shows how robustness changes as models become more complex. We compare models by computing the maximal ε against which they are robust, or equivalently, the margin for linear models, $\min_i y_i \mathbf{w}^\top \mathbf{x}_i / \|\mathbf{w}\|$. As an alternative to the margin, we estimate the maximal ε for a model by choosing a range of potential values, generating adversarial samples, and finding the largest value against which the classification error is zero. Generating adversarial samples involves optimization, and requires more implementation detail compared with computing the margin. Plots in this section are based on generating adversarial samples to match common practice in the evaluation of non-linear models. Matching margin plots are presented in Appendix E.3, which compare against the solution found using CVXPY [35] and adversarial training given the maximal ε . Our plots depict mean and error bars for 3 random seeds.

5.2 Plotting the Trade-offs

Fig. 4 illustrates the trade-off between standard accuracy and adversarial robustness. Adversarial training finds the maximally robust classifier only if it is trained with the knowledge of the maximally robust ε (Fig. 4a). Without this knowledge, we have to search for the maximal ε by training multiple models. This adds further computational complexity to adversarial training which performs an alternated optimization. In contrast, explicit regularization converges to a maximally robust classifier for a small enough regularization constant (Fig. 4b).

On CIFAR-10, we compare adversarial training with the regularization method TRADES [10] following the state-of-the-art best practices [4]. Both methods depend on a constant ε during training. Fig. 4c shows optimal robustness is achieved for a model trained and tested with the same ε . When the test ε is unknown, both methods need to search for the optimal ε . Given the optimal training ε , Fig. 4d investigates whether TRADES performs similar to an optimal linear regularization (observed in Fig. 4b), that is the optimal robustness is achieved with infinitesimal regularization. In contrast to the linear regime, the robustness degrades with smaller regularization. We hypothesize that with enough model capacity, using the optimal ε , and sufficient training iterations, smaller regularization should improve robustness. That suggests that there is potential for improvement in TRADES and better understanding of robustness in non-linear models.

5.3 CIFAR-10 Fourier- ℓ_∞ Robustness

Fig. 5 reports the maximally robust ε of image classification models on CIFAR-10. We evaluate top defenses on the leaderboard of RobustBench [5]. The attack methods are APGD-CE and APGD-DLR with default hyperparameters in RobustBench and $\varepsilon = 8/255$. Theoretical results do not provide guarantees beyond the maximally robust ε . Even robust models against corruptions with no adversarial training achieve similar robustness to ℓ_2/ℓ_∞ models. The maximal ε is the largest at which adversarial accuracy is no more than 1% worse than the standard accuracy. All models have almost zero accuracy against larger, but still perceptually small, perturbations ($\varepsilon = 20/255$). Appendix E.4 gives more examples of Fourier- ℓ_∞ attacks and band-limited variations similar to Fig. 1 for robustly trained models, showing that perturbations are qualitatively different from those against the standard model.

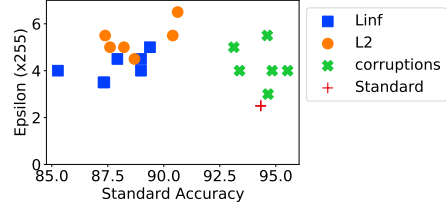


Figure 5: Maximally robust ε against Fourier- ℓ_∞ for recent defenses. Color and shape denote the type of robust training: adversarial (ℓ_2 or ℓ_∞), corruptions, or standard training. Fourier- ℓ_∞ is a strong attack against current robust models.

6 Related work

This paper bridges two bodies of work on adversarial robustness and optimization bias. As such there are many related works, the most relevant of which we discuss here. Prior works either did not connect optimization bias to adversarial robustness beyond margin-maximization [36–38] or only considered adversarial training with a given perturbation size [39].

Robustness Trade-offs Most prior work defines the metric for robustness and generalization using an expectation over the loss. Instead, we define robustness as a set of classification constraints. Our approach better matches the security perspective that even a single inaccurate prediction is a vulnerability. The limitation is explicit constraints only ensure perfect accuracy near the training set. Standard generalization remains to be studied using other approaches such with assumptions on the data distribution. Existing work has used assumptions about the data distribution to achieve explicit trade-offs between robustness and standard generalization [40–43, 7, 10, 9, 16, 8].

Fourier Analysis of Robustness. Various observations have been made about Fourier properties of adversarial perturbations against deep non-linear models [44, 23, 25]. Yin et al. [26] showed that adversarial training increases robustness to perturbations concentrated at high frequencies and reduces robustness to perturbations concentrated at low frequencies. Ortiz-Jimenez et al. [45] also observed that the measured margin of classifiers at high frequencies is larger than the margin at low frequencies. Our Corollary 2 does not distinguish between low and high frequencies but we establish an exact characterization of robustness. Caro et al. [46] hypothesized about the implicit robustness to ℓ_1 perturbations in the Fourier domain while we prove maximal robustness to Fourier- ℓ_∞ perturbations.

Architectural Robustness. An implication of our results is that robustness can be achieved at a lower computational cost compared with adversarial training by various architectural choices as recently explored [47–49]. Moreover, for architectural choices that align with human biases, standard generalization can also improve [50]. Another potential future direction is to rethink ℓ_p robustness as an architectural bias and find inspiration in human visual system for appropriate architectural choices.

Robust Optimization A robust counterpart to an optimization problem considers uncertainty in the data and optimizes for the worst-case. Ben-Tal et al. [14] provided extensive formulations and discussions on robust counterparts to various convex optimization problems. Adversarial robustness is one such robust counterpart and many other robust counterparts could also be considered in deep learning. An example is adversarial perturbations with different norm-ball constraints at different training inputs. Madry et al. [3] observed the link between robust optimization and adversarial robustness where the objective is a min-max problem that minimizes the worst-case loss. However, they did not consider the more challenging problem of maximally robust optimization that we revisit.

Implicit bias of optimization methods. Minimizing the empirical risk for an overparametrized model with more parameters than the training data has multiple solutions. Zhang et al. [51] observed that overparametrized deep models can even fit to randomly labeled training data, yet given correct labels they consistently generalize to test data. This behavior has been explained using the implicit bias of optimization methods towards particular solutions. Gunasekar et al. [12] proved that minimizing the empirical risk using steepest descent and mirror descent have an implicit bias towards minimum norm solutions in overparametrized linear classification. Characterizing the implicit bias in linear

regression proved to be more challenging and dependent on the initialization. Ji and Telgarsky [52] proved that training a deep linear classifier using gradient descent not only implicitly converges to the minimum norm classifier in the space of the product of parameters, each layer is also biased towards rank-1 matrices aligned with adjacent layers. Gunasekar et al. [22] proved the implicit bias of gradient descent in training linear convolutional classifiers is towards minimum norm solutions in the Fourier domain that depends on the number of layers. Ji and Telgarsky [53] has established the directional alignment in the training of deep linear networks using gradient flow as well as the implicit bias of training deep 2-homogeneous networks. In the case of gradient flow (gradient descent with infinitesimal step size) the implicit bias of training multi-layer linear models is towards rank-1 layers that satisfy directional alignment with adjacent layers [53, Proposition 4.4]. Recently, Yun et al. [54] has proposed a unified framework for implicit bias of neural networks using tensor formulation that includes fully-connected, diagonal, and convolutional networks and weakened the convergence assumptions.

Recent theory of generalization in deep learning, in particular the double descent phenomenon, studies the generalization properties of minimum norm solutions for finite and noisy training sets [13]. Characterization of the double descent phenomenon relies on the implicit bias of optimization methods while using additional assumptions about the data distribution. In contrast, our results only rely on the implicit bias of optimization and hence are independent of the data distribution.

Hypotheses. Goodfellow et al. [2] proposed the linearity hypothesis that informally suggests ℓ_p adversarial samples exist because deep learning models converge to functions similar to linear models. To improve robustness, they argued models have to be more non-linear. Based on our framework, linear models are not inherently weak. When trained, regularized, and parametrized appropriately they can be robust to some degree, the extent of which depends on the dataset. Gilmer et al. [55] proposed adversarial spheres as a toy example where a two layer neural network exists with perfect standard and robust accuracy for non-zero perturbations. Yet, training a randomly initialized model with gradient descent and finite data does not converge to a robust model. Based on our framework, we interpret this as an example where the implicit bias of gradient descent is not towards the ground-truth model, even though there is no misalignment in the architecture. It would be interesting to understand this implicit bias in future work.

Robustness to ℓ_p -bounded attacks. Robustness is achieved when any perturbation to natural inputs that changes a classifier’s prediction also confuses a human. ℓ_p -bounded attacks are the first step in achieving adversarial robustness. Tramer et al. [6] have recently shown many recent robust models only achieve spurious robustness against ℓ_∞ and ℓ_1 attacks. Croce and Hein [34] showed that on image classification datasets there is still a large gap in adversarial robustness to ℓ_p -bounded attacks and standard accuracy. Robustness to multiple ℓ_p -bounded perturbations through adversarial training and its trade-offs has also been analyzed [56, 57]. Sharif et al. [58], Sen et al. [59] argue that none of ℓ_0 , ℓ_1 , ℓ_∞ , or SSIM are a perfect match for human perception of similarity. That is for any such norm, for any ε , there exists a perturbation such that humans classify it differently. Attacks based on other perceptual similarity metrics exist [60, 61]. This shows that the quest for adversarial robustness should also be seen as a quest for understanding human perception.

Robustness through Regularization Various regularization methods have been proposed for adversarial robustness that penalize the gradient norm and can be studied using the framework of maximally robust classification. Lyu et al. [62] proposed general ℓ_p norm regularization of gradients. Hein and Andriushchenko [29] proposed the Cross-Lipschitz penalty by regularizing the norm of the difference between two gradient vectors of the function. Ross and Doshi-Velez [63] proposed ℓ_2 regularization of the norm of the gradients. Sokolić et al. [30] performed regularization of Frobenius norm of the per-layer Jacobian. Moosavi-Dezfooli et al. [64] proposed penalizing the curvature of the loss function. Qin et al. [31] proposed encouraging local linearity by penalizing the error of local linearity. Simon-Gabriel et al. [65] proposed regularization of the gradient norm where the dual norm of the attack norm is used. Ma et al. [66] proposed Hessian regularization. Guo et al. [32] showed that some regularization methods are equivalent or perform similarly in practice. Strong gradient or curvature regularization methods can suffer from gradient masking [66].

Certified Robustness. Adversarially trained models are empirically harder to attack than standard models. But their robustness is not often provable. Certifiably robust models seek to close this gap [29, 67–70]. A model is certifiably robust if for any input, it also provides an ε -certificate that guarantees robustness to any perturbation within the ε -ball of the input. In contrast, a maximally robust classifier finds a classifier that is guaranteed to be robust to maximal ε while classifying all

training data correctly. That allows for data dependent robustness guarantees at test time. In this work, we have not explored standard generalization guarantees.

7 Conclusion

We demonstrated that the choice of optimizer, neural network architecture, and regularizer, significantly affect the adversarial robustness of linear neural networks. These results lead us to a novel Fourier- ℓ_∞ attack with controllable spectral properties applied against deep non-linear CIFAR-10 models. Our results provide a framework, insights, and directions for improving robustness of non-linear models through approaches other than adversarial training.

Limitations. We have not proposed a novel defense for non-linear models but provided directions and insight. There are challenges in extending our theory to non-linear models that needs additional assumptions (See [Section 6](#) and [Appendix D](#)). There is a growing literature on the implicit bias of non-linear networks that can be used to extend our results [71–73]. There is a small gap in [Fig. 3](#) between theory and experiment that might be due to limited training time.

Societal Impact. We theoretically connect a security challenge to the implicit and explicit biases in machine learning, both with potential negative impacts. We show that the latter can be used to positively change the former.

Acknowledgements

The authors would like to thank Nicholas Carlini, Nicolas Papernot, and Courtney Paquette for helpful discussions and invaluable feedback. NLR is supported by the Canada CIFAR AI Chair program.

References

- [1] Christian Szegedy, Wojciech Zaremba, Ilya Sutskever, Joan Bruna, Dumitru Erhan, Ian Goodfellow, and Rob Fergus. Intriguing properties of neural networks. *arXiv preprint arXiv:1312.6199*, 2013.
- [2] Ian J Goodfellow, Jonathon Shlens, and Christian Szegedy. Explaining and harnessing adversarial examples. *arXiv preprint arXiv:1412.6572*, 2014.
- [3] Aleksander Madry, Aleksandar Makelov, Ludwig Schmidt, Dimitris Tsipras, and Adrian Vladu. Towards deep learning models resistant to adversarial attacks. *arXiv preprint arXiv:1706.06083*, 2017.
- [4] Sven Gowal, Chongli Qin, Jonathan Uesato, Timothy Mann, and Pushmeet Kohli. Uncovering the Limits of Adversarial Training against Norm-Bounded Adversarial Examples. *arXiv e-prints*, art. arXiv:2010.03593, October 2020.
- [5] Francesco Croce, Maksym Andriushchenko, Vikash Sehwal, Nicolas Flammarion, Mung Chiang, Prateek Mittal, and Matthias Hein. Robustbench: a standardized adversarial robustness benchmark. *arXiv preprint arXiv:2010.09670*, 2020.
- [6] Florian Tramèr, Nicholas Carlini, Wieland Brendel, and Aleksander Madry. On Adaptive Attacks to Adversarial Example Defenses. *arXiv e-prints*, art. arXiv:2002.08347, February 2020.
- [7] Dimitris Tsipras, Shibani Santurkar, Logan Engstrom, Alexander Turner, and Aleksander Madry. Robustness may be at odds with accuracy. *arXiv preprint arXiv:1805.12152*, 2018.
- [8] Alhussein Fawzi, Omar Fawzi, and Pascal Frossard. Analysis of classifiers’ robustness to adversarial perturbations. *Machine Learning*, 107(3):481–508, 2018.
- [9] Ludwig Schmidt, Shibani Santurkar, Dimitris Tsipras, Kunal Talwar, and Aleksander Madry. Adversarially robust generalization requires more data. In *Advances in Neural Information Processing Systems*, pages 5014–5026, 2018.
- [10] Hongyang Zhang, Yaodong Yu, Jiantao Jiao, Eric P. Xing, Laurent El Ghaoui, and Michael I. Jordan. Theoretically Principled Trade-off between Robustness and Accuracy. *arXiv e-prints*, art. arXiv:1901.08573, January 2019.

- [11] Chiyuan Zhang, Samy Bengio, Moritz Hardt, Benjamin Recht, and Oriol Vinyals. Understanding deep learning requires rethinking generalization. *arXiv preprint arXiv:1611.03530*, 2016.
- [12] Suriya Gunasekar, Jason Lee, Daniel Soudry, and Nathan Srebro. [Characterizing implicit bias in terms of optimization geometry](#). *arXiv preprint arXiv:1802.08246*, 2018.
- [13] Trevor Hastie, Andrea Montanari, Saharon Rosset, and Ryan J. Tibshirani. Surprises in High-Dimensional Ridgeless Least Squares Interpolation. *arXiv e-prints*, art. arXiv:1903.08560, March 2019.
- [14] Aharon Ben-Tal, Laurent El Ghaoui, and Arkadi Nemirovski. *Robust optimization*, volume 28. Princeton University Press, 2009.
- [15] Tom B. Brown, Dandelion Mané, Aurko Roy, Martín Abadi, and Justin Gilmer. Adversarial Patch. *arXiv e-prints*, art. arXiv:1712.09665, December 2017.
- [16] Alhussein Fawzi, Hamza Fawzi, and Omar Fawzi. Adversarial vulnerability for any classifier. In *Advances in neural information processing systems*, pages 1178–1187, 2018.
- [17] John Shawe-Taylor, Peter L. Bartlett, Robert C. Williamson, and Martin Anthony. Structural risk minimization over data-dependent hierarchies. *IEEE Trans. Inf. Theory*, 44(5):1926–1940, 1998.
- [18] Matus Telgarsky. Margins, shrinkage, and boosting. In *ICML (2)*, volume 28 of *JMLR Workshop and Conference Proceedings*, pages 307–315. JMLR.org, 2013.
- [19] Preetum Nakkiran, Gal Kaplun, Yamini Bansal, Tristan Yang, Boaz Barak, and Ilya Sutskever. Deep double descent: Where bigger models and more data hurt. *CoRR*, abs/1912.02292, 2019. URL <http://arxiv.org/abs/1912.02292>.
- [20] Stephen Boyd and Lieven Vandenberghe. *Convex optimization*. Cambridge university press, 2004.
- [21] Mor Shpigel Nacson, Jason Lee, Suriya Gunasekar, Pedro Henrique Pamplona Savarese, Nathan Srebro, and Daniel Soudry. Convergence of gradient descent on separable data. In *The 22nd International Conference on Artificial Intelligence and Statistics*, pages 3420–3428. PMLR, 2019.
- [22] Suriya Gunasekar, Jason D Lee, Daniel Soudry, and Nati Srebro. Implicit bias of gradient descent on linear convolutional networks. In *Advances in Neural Information Processing Systems*, pages 9461–9471, 2018.
- [23] Yusuke Tsuzuku and Issei Sato. On the structural sensitivity of deep convolutional networks to the directions of fourier basis functions. In *Proceedings of the IEEE Conference on Computer Vision and Pattern Recognition*, pages 51–60, 2019.
- [24] Chuan Guo, Jared S. Frank, and Kilian Q. Weinberger. Low frequency adversarial perturbation. In Amir Globerson and Ricardo Silva, editors, *Proceedings of the Thirty-Fifth Conference on Uncertainty in Artificial Intelligence, UAI 2019, Tel Aviv, Israel, July 22-25, 2019*, volume 115 of *Proceedings of Machine Learning Research*, pages 1127–1137. AUAI Press, 2019. URL <http://proceedings.mlr.press/v115/guo20a.html>.
- [25] Yash Sharma, Gavin Weiguang Ding, and Marcus Brubaker. On the effectiveness of low frequency perturbations. *arXiv preprint arXiv:1903.00073*, 2019.
- [26] Dong Yin, Raphael Gontijo Lopes, Jon Shlens, Ekin Dogus Cubuk, and Justin Gilmer. A Fourier perspective on model robustness in computer vision. *Advances in Neural Information Processing Systems*, 32:13276–13286, 2019.
- [27] Saharon Rosset, Ji Zhu, and Trevor J Hastie. Margin maximizing loss functions. In *Advances in neural information processing systems*, pages 1237–1244, 2004.
- [28] Colin Wei, Jason D Lee, Qiang Liu, and Tengyu Ma. Regularization matters: Generalization and optimization of neural nets vs their induced kernel. In *Advances in Neural Information Processing Systems*, pages 9712–9724, 2019.

- [29] Matthias Hein and Maksym Andriushchenko. Formal guarantees on the robustness of a classifier against adversarial manipulation. In *Advances in neural information processing systems*, pages 2266–2276, 2017.
- [30] Jure Sokolić, Raja Giryes, Guillermo Sapiro, and Miguel RD Rodrigues. Robust large margin deep neural networks. *IEEE Transactions on Signal Processing*, 65(16):4265–4280, 2017.
- [31] Chongli Qin, James Martens, Sven Gowal, Dilip Krishnan, Krishnamurthy Dvijotham, Alhussein Fawzi, Soham De, Robert Stanforth, and Pushmeet Kohli. Adversarial robustness through local linearization. In *Advances in Neural Information Processing Systems*, pages 13847–13856, 2019.
- [32] Yiwen Guo, Long Chen, Yurong Chen, and Changshui Zhang. On connections between regularizations for improving dnn robustness. *IEEE transactions on pattern analysis and machine intelligence*, 2020.
- [33] Alex Krizhevsky, Geoffrey Hinton, et al. Learning multiple layers of features from tiny images. 2009.
- [34] Francesco Croce and Matthias Hein. Reliable evaluation of adversarial robustness with an ensemble of diverse parameter-free attacks. In *ICML*, volume 119 of *Proceedings of Machine Learning Research*, pages 2206–2216. PMLR, 2020.
- [35] Steven Diamond and Stephen Boyd. CVXPY: A Python-embedded modeling language for convex optimization. *Journal of Machine Learning Research*, 17(83):1–5, 2016.
- [36] Linhai Ma and Liang Liang. Increasing-margin adversarial (IMA) training to improve adversarial robustness of neural networks. *CoRR*, abs/2005.09147, 2020. URL <https://arxiv.org/abs/2005.09147>.
- [37] Gavin Weiguang Ding, Yash Sharma, Kry Yik Chau Lui, and Ruitong Huang. Max-margin adversarial (MMA) training: Direct input space margin maximization through adversarial training. *CoRR*, abs/1812.02637, 2018. URL <http://arxiv.org/abs/1812.02637>.
- [38] Gamaleldin F. Elsayed, Dilip Krishnan, Hossein Mobahi, Kevin Regan, and Samy Bengio. Large margin deep networks for classification, 2018.
- [39] Yan Li, Ethan X Fang, Huan Xu, and Tuo Zhao. Implicit bias of gradient descent based adversarial training on separable data. In *International Conference on Learning Representations*, 2019.
- [40] Edgar Dobriban, Hamed Hassani, David Hong, and Alexander Robey. Provable tradeoffs in adversarially robust classification. *arXiv e-prints*, art. arXiv:2006.05161, June 2020.
- [41] Adel Javanmard and Mahdi Soltanolkotabi. Precise Statistical Analysis of Classification Accuracies for Adversarial Training. *arXiv e-prints*, art. arXiv:2010.11213, October 2020.
- [42] Adel Javanmard, Mahdi Soltanolkotabi, and Hamed Hassani. Precise tradeoffs in adversarial training for linear regression. In *COLT*, volume 125 of *Proceedings of Machine Learning Research*, pages 2034–2078. PMLR, 2020.
- [43] Aditi Raghunathan, Sang Michael Xie, Fanny Yang, John Duchi, and Percy Liang. Understanding and mitigating the tradeoff between robustness and accuracy. *arXiv preprint arXiv:2002.10716*, 2020.
- [44] Andrew Ilyas, Shibani Santurkar, Dimitris Tsipras, Logan Engstrom, Brandon Tran, and Aleksander Madry. Adversarial examples are not bugs, they are features. In *Advances in Neural Information Processing Systems*, pages 125–136, 2019.
- [45] Guillermo Ortiz-Jimenez, Apostolos Modas, Seyed-Mohsen Moosavi-Dezfooli, and Pascal Frossard. Hold me tight! influence of discriminative features on deep network boundaries. *arXiv preprint arXiv:2002.06349*, 2020.

- [46] Josue Ortega Caro, Yilong Ju, Ryan Pyle, and Ankit Patel. Using learning dynamics to explore the role of implicit regularization in adversarial examples. *arXiv preprint arXiv:2006.11440*, 2020.
- [47] Cihang Xie, Mingxing Tan, Boqing Gong, Alan L. Yuille, and Quoc V. Le. Smooth adversarial training. *CoRR*, abs/2006.14536, 2020.
- [48] Angus Galloway, Anna Golubeva, Thomas Tanay, Medhat Moussa, and Graham W. Taylor. Batch normalization is a cause of adversarial vulnerability. *CoRR*, abs/1905.02161, 2019.
- [49] Muhammad Awais, Fahad Shamshad, and Sung-Ho Bae. Towards an adversarially robust normalization approach. *CoRR*, abs/2006.11007, 2020.
- [50] Cristina Vasconcelos, Hugo Larochelle, Vincent Dumoulin, Nicolas Le Roux, and Ross Goroshin. An effective anti-aliasing approach for residual networks. *CoRR*, abs/2011.10675, 2020.
- [51] Chiyuan Zhang, Samy Bengio, Moritz Hardt, Benjamin Recht, and Oriol Vinyals. Understanding deep learning requires rethinking generalization. In *ICLR*. OpenReview.net, 2017.
- [52] Ziwei Ji and Matus Telgarsky. Gradient descent aligns the layers of deep linear networks. *arXiv preprint arXiv:1810.02032*, 2018.
- [53] Ziwei Ji and Matus Telgarsky. Directional convergence and alignment in deep learning. In *NeurIPS*, 2020.
- [54] Chulhee Yun, Shankar Krishnan, and Hossein Mobahi. A Unifying View on Implicit Bias in Training Linear Neural Networks. *arXiv e-prints*, art. arXiv:2010.02501, October 2020.
- [55] Justin Gilmer, Luke Metz, Fartash Faghri, Samuel S. Schoenholz, Maithra Raghu, Martin Wattenberg, and Ian Goodfellow. Adversarial Spheres. *arXiv e-prints*, art. arXiv:1801.02774, January 2018.
- [56] Florian Tramèr and Dan Boneh. Adversarial training and robustness for multiple perturbations. In *NeurIPS*, pages 5858–5868, 2019.
- [57] Pratyush Maini, Eric Wong, and Zico Kolter. Adversarial robustness against the union of multiple perturbation models. In *International Conference on Machine Learning*, pages 6640–6650. PMLR, 2020.
- [58] Mahmood Sharif, Lujo Bauer, and Michael K. Reiter. On the suitability of lp-norms for creating and preventing adversarial examples. In *CVPR Workshops*, pages 1605–1613. IEEE Computer Society, 2018.
- [59] Ayon Sen, Xiaojin Zhu, Liam Marshall, and Robert Nowak. Should Adversarial Attacks Use Pixel p-Norm? *arXiv e-prints*, art. arXiv:1906.02439, June 2019.
- [60] Zhengyu Zhao, Zhuoran Liu, and Martha Larson. Adversarial Color Enhancement: Generating Unrestricted Adversarial Images by Optimizing a Color Filter. *arXiv e-prints*, art. arXiv:2002.01008, February 2020.
- [61] Hsueh-Ti Derek Liu, Michael Tao, Chun-Liang Li, Derek Nowrouzezahrai, and Alec Jacobson. Beyond pixel norm-balls: Parametric adversaries using an analytically differentiable renderer. In *ICLR (Poster)*. OpenReview.net, 2019.
- [62] Chunchuan Lyu, Kaizhu Huang, and Hai-Ning Liang. A unified gradient regularization family for adversarial examples. In *2015 IEEE International Conference on Data Mining*, pages 301–309. IEEE, 2015.
- [63] Andrew Ross and Finale Doshi-Velez. Improving the adversarial robustness and interpretability of deep neural networks by regularizing their input gradients. In *Proceedings of the AAAI Conference on Artificial Intelligence*, volume 32, 2018.

- [64] Seyed-Mohsen Moosavi-Dezfooli, Alhussein Fawzi, Jonathan Uesato, and Pascal Frossard. Robustness via curvature regularization, and vice versa. In *Proceedings of the IEEE Conference on Computer Vision and Pattern Recognition*, pages 9078–9086, 2019.
- [65] Carl-Johann Simon-Gabriel, Yann Ollivier, Leon Bottou, Bernhard Schölkopf, and David Lopez-Paz. First-order adversarial vulnerability of neural networks and input dimension. In *International Conference on Machine Learning*, pages 5809–5817. PMLR, 2019.
- [66] Avery Ma, Fartash Faghri, and Amir-massoud Farahmand. Adversarial Robustness through Regularization: A Second-Order Approach. *arXiv e-prints*, art. arXiv:2004.01832, April 2020.
- [67] Eric Wong and Zico Kolter. Provable defenses against adversarial examples via the convex outer adversarial polytope. In *International Conference on Machine Learning*, pages 5286–5295. PMLR, 2018.
- [68] Jeremy M Cohen, Elan Rosenfeld, and J Zico Kolter. Certified adversarial robustness via randomized smoothing. *arXiv preprint arXiv:1902.02918*, 2019.
- [69] Sven Gowal, Krishnamurthy Dvijotham, Robert Stanforth, Rudy Bunel, Chongli Qin, Jonathan Uesato, Relja Arandjelovic, Timothy Mann, and Pushmeet Kohli. On the Effectiveness of Interval Bound Propagation for Training Verifiably Robust Models. *arXiv e-prints*, art. arXiv:1810.12715, October 2018.
- [70] Hadi Salman, Greg Yang, Huan Zhang, Cho-Jui Hsieh, and Pengchuan Zhang. A convex relaxation barrier to tight robustness verification of neural networks. In *Advances in Neural Information Processing Systems*, pages 9835–9846, 2019.
- [71] Lenaic Chizat and Francis Bach. Implicit bias of gradient descent for wide two-layer neural networks trained with the logistic loss. In *Conference on Learning Theory*, pages 1305–1338. PMLR, 2020.
- [72] Kaifeng Lyu and Jian Li. Gradient descent maximizes the margin of homogeneous neural networks. In *ICLR*. OpenReview.net, 2020.
- [73] Greg Ongie, Rebecca Willett, Daniel Soudry, and Nathan Srebro. A function space view of bounded norm infinite width relu nets: The multivariate case. In *ICLR*. OpenReview.net, 2020.
- [74] Anish Athalye, Nicholas Carlini, and David Wagner. Obfuscated gradients give a false sense of security: Circumventing defenses to adversarial examples. *arXiv preprint arXiv:1802.00420*, 2018.
- [75] Andrea Montanari, Feng Ruan, Youngtak Sohn, and Jun Yan. The generalization error of max-margin linear classifiers: High-dimensional asymptotics in the overparametrized regime. *arXiv preprint arXiv:1911.01544*, 2019.
- [76] Zeyu Deng, Abba Kammoun, and Christos Thrampoulidis. A Model of Double Descent for High-dimensional Binary Linear Classification. *arXiv e-prints*, art. arXiv:1911.05822, November 2019.
- [77] Neal Parikh and Stephen Boyd. [Proximal algorithms](#). *Foundations and Trends in Optimization*, 2013.
- [78] Nicholas Carlini and David Wagner. Towards evaluating the robustness of neural networks. In *2017 IEEE Symposium on Security and Privacy (SP)*, pages 39–57. IEEE, 2017.
- [79] Yair Carmon, Aditi Raghunathan, Ludwig Schmidt, John C. Duchi, and Percy Liang. Unlabeled data improves adversarial robustness. In *NeurIPS*, pages 11190–11201, 2019.
- [80] Maximilian Augustin, Alexander Meinke, and Matthias Hein. Adversarial robustness on in- and out-distribution improves explainability. In *European Conference on Computer Vision*, pages 228–245. Springer, 2020.
- [81] Francis Bach, Rodolphe Jenatton, Julien Mairal, Guillaume Obozinski, et al. Structured sparsity through convex optimization. *Statistical Science*, 27(4):450–468, 2012.

A Generalization of the Maximally Robust Classifier

Definition A.1 (Maximally Robust Classifier with Slack Loss). Let $\xi \geq 0$ denote a given slack variable. A maximally robust classifier with slack loss is the solution to

$$\arg \max_{\varphi \in \Phi} \left\{ \varepsilon \mid \mathbb{E}_{(\mathbf{x}, y)} \max_{\|\boldsymbol{\delta}\| \leq \varepsilon} \zeta(y\varphi(\mathbf{x} + \boldsymbol{\delta})) \leq \xi \right\}. \quad (11)$$

This formulation is similar to the saddle-point problem in that we seek to minimize the expectation of the worst case loss. The difference is that we also seek to maximize ε . However, we have introduced another arbitrary variable ξ that is not optimized as part of the problem. For linear classifiers and the hinge loss, $\zeta(z) = [1 - z]_+$, Eq. (11) can be written as,

$$\arg \max_{\mathbf{w}} \left\{ \varepsilon \mid \mathbb{E}_{(\mathbf{x}, y)} [1 - y\mathbf{w}^\top \mathbf{x} + \varepsilon \|\mathbf{w}\|_*]_+ \leq \xi \right\}, \quad (12)$$

where $[\cdot]_+$ is the hinge loss, and the weight penalty term $\|\mathbf{w}\|_*$ is inside the hinge loss. This subtle difference makes solving the problem more challenging than weight penalty outside the loss.

Because of the two challenges we noted, we do not study the maximal robustness with slack loss.

B Proofs

B.1 Proof of Lemma 2.1

Proof. We first show that the maximally robust classifier is equivalent to a robust counterpart by removing $\boldsymbol{\delta}$ from the problem,

$$\begin{aligned} & \arg \max_{\mathbf{w}, b} \{ \varepsilon \mid y_i(\mathbf{w}^\top (\mathbf{x}_i + \boldsymbol{\delta}) + b) > 0, \forall i, \|\boldsymbol{\delta}\| \leq \varepsilon \} \\ & \quad \text{(homogeneity of } p\text{-norm)} \\ & = \arg \max_{\mathbf{w}, b} \{ \varepsilon \mid y_i(\mathbf{w}^\top (\mathbf{x}_i + \varepsilon \boldsymbol{\delta}) + b) > 0, \forall i, \|\boldsymbol{\delta}\| \leq 1 \} \\ & \quad \text{(if it is true for all } \boldsymbol{\delta} \text{ it is true for the worst of them)} \\ & = \arg \max_{\mathbf{w}, b} \{ \varepsilon \mid \inf_{\|\boldsymbol{\delta}\| \leq 1} y_i(\mathbf{w}^\top (\mathbf{x}_i + \varepsilon \boldsymbol{\delta}) + b) > 0, \forall i \} \\ & = \arg \max_{\mathbf{w}, b} \{ \varepsilon \mid y_i(\mathbf{w}^\top \mathbf{x}_i + b) + \varepsilon \inf_{\|\boldsymbol{\delta}\| \leq 1} \mathbf{w}^\top \boldsymbol{\delta} > 0, \forall i \} \\ & \quad \text{(definition of dual norm)} \\ & = \arg \max_{\mathbf{w}, b} \{ \varepsilon \mid y_i(\mathbf{w}^\top \mathbf{x}_i + b) > \varepsilon \|\mathbf{w}\|_*, \forall i \} \end{aligned}$$

Assuming $\mathbf{w} \neq 0$, which is a result of linear separability assumption, we can divide both sides by $\|\mathbf{w}\|_*$ and change variables,

$$= \arg \max_{\mathbf{w}, b} \{ \varepsilon \mid y_i(\mathbf{w}^\top \mathbf{x}_i + b) \geq \varepsilon, \forall i, \|\mathbf{w}\|_* \leq 1 \},$$

where we are also allowed to change $>$ to \geq because any solution to one problem gives an equivalent solution to the other given $\mathbf{w} \neq 0$.

Now we show that the robust counterpart is equivalent to the minimum norm classification problem by removing ε . When the data is linearly separable there exists a solution with $\varepsilon > 0$,

$$\begin{aligned} & \arg \max_{\mathbf{w}, b} \{ \varepsilon \mid y_i(\mathbf{w}^\top \mathbf{x}_i + b) > \varepsilon \|\mathbf{w}\|_*, \forall i \} \\ & = \arg \max_{\mathbf{w}, b} \left\{ \varepsilon \mid y_i \left(\frac{\mathbf{w}^\top}{\varepsilon \|\mathbf{w}\|_*} \mathbf{x}_i + \frac{b}{\varepsilon \|\mathbf{w}\|_*} \right) \geq 1, \forall i \right\} \end{aligned}$$

This problem is invariant to any non-zero scaling of (\mathbf{w}, b) , so with no loss of generality we set $\|\mathbf{w}\|_* = 1$.

$$= \arg \max_{\mathbf{w}, b} \left\{ \varepsilon \mid y_i \left(\frac{\mathbf{w}^\top}{\varepsilon} \mathbf{x}_i + b \right) \geq 1, \forall i, \|\mathbf{w}\|_* = 1 \right\}$$

Let $\mathbf{w}' = \mathbf{w}/\varepsilon$, then the solution to the following problem gives a solution for \mathbf{w} ,

$$\begin{aligned} & \arg \max_{\mathbf{w}', b} \left\{ \frac{1}{\|\mathbf{w}'\|_*} \mid y_i(\mathbf{w}'^\top \mathbf{x}_i + b) \geq 1, \forall i \right\} \\ &= \arg \min_{\mathbf{w}', b} \left\{ \|\mathbf{w}'\|_* \mid y_i(\mathbf{w}'^\top \mathbf{x}_i + b) \geq 1, \forall i \right\}. \end{aligned}$$

□

B.2 Proof of Maximally Robust to Perturbations Bounded in Fourier Domain (Corollary 2)

The proof mostly follows from the equivalence for linear models in [Appendix B.1](#) by substituting the dual norm of Fourier- ℓ_1 . Here, \mathbf{A}^* denotes the complex conjugate transpose, $\langle \mathbf{u}, \mathbf{v} \rangle = \mathbf{u}^\top \mathbf{v}^*$ is the complex inner product, $[\mathbf{F}]_{ik} = \frac{1}{\sqrt{D}} \omega_D^{ik}$ the DFT matrix where $\omega_D = e^{-j2\pi/D}$, $j = \sqrt{-1}$.

Let $\|\cdot\|$ be a norm on \mathbb{C}^n and $\langle \cdot, \cdot \rangle$ be the complex inner product. Similar to \mathbb{R}^n , the associated dual norm is defined as $\|\delta\|_* = \sup_{\mathbf{x}} \{ |\langle \delta, \mathbf{x} \rangle| \mid \|\mathbf{x}\| \leq 1 \}$.

$$\begin{aligned} & \|\mathcal{F}(\mathbf{w})\|_1 \\ &= \sup_{\|\delta\|_\infty \leq 1} |\langle \mathcal{F}(\mathbf{w}), \delta \rangle| \\ & \quad \text{(Expressing DFT as a linear transformation.)} \\ &= \sup_{\|\delta\|_\infty \leq 1} |\langle \mathbf{F}\mathbf{w}, \delta \rangle| \\ &= \sup_{\|\delta\|_\infty \leq 1} |\langle \mathbf{w}, \mathbf{F}^* \delta \rangle| \\ & \quad \text{(Change of variables and } \mathbf{F}^{-1} = \mathbf{F}^* \text{.)} \\ &= \sup_{\|\mathbf{F}\delta\|_\infty \leq 1} |\langle \mathbf{w}, \delta \rangle| \\ &= \sup_{\|\mathcal{F}(\delta)\|_\infty \leq 1} |\langle \mathbf{w}, \delta \rangle|. \end{aligned}$$

C Linear Operations in Discrete Fourier Domain

Finding an adversarial sample with bounded Fourier- ℓ_∞ involves ℓ_∞ complex projection to ensure adversarial samples are bounded, as well as the steepest ascent direction w.r.t the Fourier- ℓ_∞ norm. We also use the complex projection onto ℓ_∞ simplex for proximal gradient method that minimizes the regularized empirical risk.

C.1 ℓ_∞ Complex Projection

Let \mathbf{v} denote the ℓ_2 projection of $\mathbf{x} \in \mathbb{C}^d$ onto the ℓ_∞ unit ball. It can be computed as,

$$\arg \min_{\|\mathbf{v}\|_\infty \leq 1} \frac{1}{2} \|\mathbf{v} - \mathbf{x}\|_2^2 \tag{13}$$

$$= \{ \mathbf{v} : \forall i, \mathbf{v}_i = \arg \min_{|\mathbf{v}_i| \leq 1} \frac{1}{2} |\mathbf{v}_i - \mathbf{x}_i|^2 \}, \tag{14}$$

that is independent projection per coordinate which can be solved by 2D projections onto ℓ_2 the unit ball in the complex plane.

C.2 Steepest Ascent Direction w.r.t. Fourier- ℓ_∞

Consider the following optimization problem,

$$\arg \max_{\mathbf{v}: \|\mathbf{F}\mathbf{v}\|_\infty \leq 1} f(\mathbf{v}), \quad (15)$$

where $\mathbf{F} \in \mathbb{C}^{d \times d}$ is the Discrete Fourier Transform (DFT) matrix and $\mathbf{F}^* = \mathbf{F}^{-1}$ and \mathbf{F}^* is the conjugate transpose.

Normalized steepest descent direction is defined as (See Boyd and Vandenberghe [20, Section 9.4]),

$$\arg \min_{\mathbf{v}} \{ \nabla \langle f(\mathbf{w}), \mathbf{v} \rangle : \|\mathbf{v}\| = 1 \}. \quad (16)$$

Similarly, we can define the steepest ascent direction,

$$\arg \max_{\mathbf{v} \in \mathbb{R}^d} \{ |\langle \nabla f(\mathbf{w}), \mathbf{v} \rangle| : \|\mathbf{F}\mathbf{v}\|_\infty = 1 \} \quad (17)$$

$$\text{(Assuming } f \text{ is linear.)} \quad (18)$$

$$\arg \max_{\mathbf{v} \in \mathbb{R}^d} \{ |\langle \mathbf{g}, \mathbf{F}^* \mathbf{F} \mathbf{v} \rangle| : \|\mathbf{F}\mathbf{v}\|_\infty = 1 \} \quad (19)$$

$$\arg \max_{\mathbf{v} \in \mathbb{R}^d} \{ |\langle \mathbf{F}\mathbf{g}, \mathbf{F}\mathbf{v} \rangle| : \|\mathbf{F}\mathbf{v}\|_\infty = 1 \} \quad (20)$$

where $\mathbf{g} = \nabla f(\mathbf{w})$.

Consider the change of variable $\mathbf{u} = \mathbf{F}\mathbf{v} \in \mathbb{C}^{d \times d}$. Since \mathbf{v} is a real vector its DFT is Hermitian, i.e. $\mathbf{u}_i^* = [\mathbf{u}]_{-i}$ for all coordinates i where $\bar{j} = j \bmod d$. Similarly, $\mathbf{F}\mathbf{g}$ is Hermitian.

$$\arg \max_{\mathbf{u} \in \mathbb{C}^d: \|\mathbf{u}\|_\infty = 1} \{ |\langle \mathbf{F}\mathbf{g}, \mathbf{u} \rangle| : \mathbf{u}_i^* = [\mathbf{u}]_{-i} \} \quad (21)$$

$$\arg \max_{\mathbf{u} \in \mathbb{C}^d: \forall i, |\mathbf{u}_i| = 1} \{ |[\mathbf{F}\mathbf{g}]_i \mathbf{u}_i| + |[\mathbf{F}\mathbf{g}]_{-i} \mathbf{u}_i^*| : \mathbf{u}_i^* = [\mathbf{u}]_{-i} \} \quad (22)$$

$$\arg \max_{\mathbf{u} \in \mathbb{C}^d: \forall i, |\mathbf{u}_i| = 1} \{ |[\mathbf{F}\mathbf{g}]_i \mathbf{u}_i| + |[\mathbf{F}\mathbf{g}]_i^* \mathbf{u}_i^*| : \mathbf{u}_i^* = [\mathbf{u}]_{-i} \} \quad (23)$$

$$\arg \max_{\mathbf{u} \in \mathbb{C}^d: \forall i, |\mathbf{u}_i| = 1} \{ |[\mathbf{F}\mathbf{g}]_i \mathbf{u}_i| : \mathbf{u}_i^* = [\mathbf{u}]_{-i} \} \quad (24)$$

$$\mathbf{u}_i = [\mathbf{F}\mathbf{g}]_i / |[\mathbf{F}\mathbf{g}]_i|. \quad (25)$$

and the steepest ascent direction is $\mathbf{v}_i = \mathbf{F}^{-1} \mathbf{u}_i$ which is a real vector. In practice, there can be non-zero small imaginary parts as numerical errors which we remove.

D Non-linear Maximally Robust Classifiers

Recall that the definition of a maximally robust classifier (Definition 2.1) handles non-linear families of functions, Φ :

$$\arg \max_{\varphi \in \Phi} \{ \varepsilon : y_i \varphi(\mathbf{x}_i + \boldsymbol{\delta}) > 0, \forall i, \|\boldsymbol{\delta}\| \leq \varepsilon \}.$$

Here we extend the proof in Lemma 2.1 that made the maximally robust classification tractable by removing $\boldsymbol{\delta}$ and ε from the problem. In linking a maximally robust classifier to a minimum norm classifier when there exists a non-linear transformation, the first step that requires attention is the following,

$$\begin{aligned} & \arg \max_{\varphi \in \Phi} \{ \varepsilon : \inf_{\|\boldsymbol{\delta}\| \leq 1} y_i \varphi(\mathbf{x}_i + \varepsilon \boldsymbol{\delta}) > 0, \forall i \} \\ & \neq \arg \max_{\varphi \in \Phi} \{ \varepsilon : y_i \varphi(\mathbf{x}_i) + \varepsilon \inf_{\|\boldsymbol{\delta}\| \leq 1} \varphi(\boldsymbol{\delta}) > 0, \forall i \} \end{aligned}$$

Lemma D.1 (Gradient Norm Weighted Maximum Margin). *Let Φ be a family of locally linear classifiers near training data, i.e.*

$$\begin{aligned} \Phi &= \{ \varphi : \exists \xi > 0, \forall i, \|\boldsymbol{\delta}\| \leq 1, \varepsilon \in [0, \xi), \\ & \varphi(\mathbf{x}_i + \varepsilon \boldsymbol{\delta}) = \varphi(\mathbf{x}_i) + \varepsilon \boldsymbol{\delta}^\top \frac{\partial}{\partial \mathbf{x}} \varphi(\mathbf{x}_i) \}. \end{aligned}$$

Then a maximally robust classifier is a solution to the following problem,

$$\arg \max_{\varphi \in \Phi, \varepsilon \leq \xi} \{ \varepsilon : y_i \varphi(\mathbf{x}_i) > \varepsilon \left\| \frac{\partial}{\partial \mathbf{x}} \varphi(\mathbf{x}_i) \right\|_*, \forall i \}.$$

Proof.

$$\begin{aligned} & \arg \max_{\varphi} \{ \varepsilon : \inf_{\|\boldsymbol{\delta}\| \leq 1} y_i \varphi(\mathbf{x}_i + \varepsilon \boldsymbol{\delta}) \geq 0, \forall i \} \\ & \quad \text{(Taylor approx.)} \\ & = \arg \max_{\varphi} \{ \varepsilon : \inf_{\|\boldsymbol{\delta}\| \leq 1} y_i \varphi(\mathbf{x}_i) + y_i \varepsilon \boldsymbol{\delta}^T \frac{\partial}{\partial \mathbf{x}} \varphi(\mathbf{x}_i) \geq 0, \forall i \} \\ & = \arg \max_{\varphi} \{ \varepsilon : y_i \varphi(\mathbf{x}_i) + \varepsilon \inf_{\|\boldsymbol{\delta}\| \leq 1} \boldsymbol{\delta}^T \frac{\partial}{\partial \mathbf{x}} \varphi(\mathbf{x}_i) \geq 0, \forall i \} \\ & \quad \text{(Dual to the local derivative.)} \\ & = \arg \max_{\varphi} \{ \varepsilon : y_i \varphi(\mathbf{x}_i) \geq \varepsilon \left\| \frac{\partial}{\partial \mathbf{x}} \varphi(\mathbf{x}_i) \right\|_*, \forall i \} \\ & \quad \text{(Assuming constant gradient norm near data.)} \\ & = \arg \max_{\varphi : \left\| \frac{\partial}{\partial \mathbf{x}} \varphi(\mathbf{x}) \right\|_* \leq 1} \{ \varepsilon : y_i \varphi(\mathbf{x}_i) \geq \varepsilon, \forall i \}. \end{aligned}$$

□

The equivalence in [Lemma D.1](#) fails when Φ includes functions with non-zero higher order derivatives within the ε of the maximally robust classifier. In practice, this failure manifests itself as various forms of gradient masking or gradient obfuscation where the model has almost zero gradient near the data but large higher-order derivatives [\[74\]](#).

Various regularization methods have been proposed for adversarial robustness that penalize the gradient norm and can be studied using the framework of maximally robust classification [\[63, 65, 66, 64\]](#) Strong gradient or curvature regularization methods can suffer from gradient masking [\[66\]](#).

For general family of non-linear functions, the interplay with implicit bias of optimization and regularization methods remains to be characterized. The solution to the regularized problem in [Definition 4.1](#) is not necessarily unique. In such cases, the implicit bias of the optimizer biases the robustness.

E Extended Experiments

E.1 Details of Linear Classification Experiments

For experiments with linear classifiers, we sample n training data points from the $\mathcal{N}(0, \mathbb{I}_d)$, d -dimensional standard normal distribution centered at zero. We label data points $y = \text{sign}(\mathbf{w}^\top \mathbf{x})$, using a ground-truth linear separator sampled from $\mathcal{N}(0, \mathbb{I}_d)$. For $n < d$, the generated training data is linearly separable. This setting is similar to a number of recent theoretical works on the implicit bias of optimization methods in deep learning and specifically the double descent phenomenon in generalization [\[75, 76\]](#). We focus on robustness against norm-bounded attacks centered at the training data, in particular, ℓ_2 , ℓ_∞ , ℓ_1 and Fourier- ℓ_∞ bounded attacks.

Because the constraints and the objective in the minimum norm linear classification problem are convex, we can use off-the-shelf convex optimization toolbox to find the solution for small enough d and n . We use the CVXPY library [\[35\]](#). We evaluate the following approaches based on the implicit bias of optimization: Gradient Descent (GD), Coordinate Descent (CD), and Sign Gradient Descent (SignGD) on fully-connected networks as well as GD on linear two-layer convolutional networks (discussed in [Section 3](#)). We also compare with explicit regularization methods (discussed in [Section 4](#)) trained using proximal gradient methods [\[77\]](#). We do not use gradient descent because ℓ_p norms can be non-differentiable at some points (e.g. ℓ_1 and ℓ_∞) and we seek a global minima of the regularized empirical risk. We also compare with adversarial training. As we discussed in [Section 2.1](#) we need to provide the value of maximally robust ε to adversarial training for finding

Hyperparameter	Values
Random seed	0,1,2
d	100
d/n	1, 2, 4, 8, 16, 32
Training steps	10000
Learning rate	1e-5, 3e-5, 1e-4, 3e-4, 1e-3, 3e-3, 1e-2, 3e-2, 1e-1, 3e-1, 1, 2, 3, 6, 9, 10, 20, 30, 50
Reg. coefficient	1e-7, 1e-6, 1e-5, 1e-4, 1e-3, 1e-2, 1e-1, 1, 10, 3e-3, 5e-3, 3e-2, 5e-2, 3e-1, 5e-1
Line search max step	1, 10, 100, 1000
Adv. Train steps	10
Adv. Train learning rate	0.1
Runtime (line search/prox. method)	< 20 minutes
Runtime (others)	< 2 minutes

Table 1: **Range of Hyperparameters.** Each run uses 2 CPU cores.

a maximally robust classifier. In our experiments, we give an advantage to adversarial training by providing it with the maximally robust ε . We also use the steepest descent direction corresponding to the attack norm to solve the inner maximization.

For regularization methods a sufficiently small regularization coefficient achieves maximal robustness. Adversarial training given the maximal ε also converges to the same solution. We tune all hyperparameters for all methods including learning rate regularization coefficient and maximum step size in line search. We provide a list of values in Table 1.

E.2 Details of CIFAR-10 experiments

For Figs. 4c and 4d, the model is a WRN-28-10. We use SGD momentum (momentum set to 0.9) with a learning rate schedule that warms up from 0 to LR for 10 epochs, then decays slowly using a cosine schedule back to zero over 200 epochs. LR is set to $0.1 * BS / 256$, where batch size, BS, is set to 1024. Experiments runs on Google Cloud TPUv3 over 32 cores. All models are trained from scratch and uses the default initialization from JAX/Haiku. We use the KL loss and typical adversarial loss for adversarial training. The inner optimization either maximizes the KL divergence (for TRADES) or the cross-entropy loss (for AT) and we use Adam with a step-size of 0.1.

For the evaluation, we use 40 PGD steps (with Adam as the underlying optimizer and step-size 0.1). Instead of optimizing the cross-entropy loss, we used the margin-loss [78].

For Fig. 5, we evaluate the models in Table 2 against our Fourier- ℓ_p attack with varying ε in the range $[0, 8] \times 255$ with step size 0.5. We report the largest ε at which the robust test accuracy is at most 1% lower than standard test accuracy of the model. We run the attack for 20 iterations with no restarts and use apgd-ce, and apgd-dlr methods from AutoAttack.

E.3 Margin Figures

A small gap exists between the solution found using CVXPY compared with coordinate descent. That is because of limited number of training iterations. The convergence of coordinate descent to minimum ℓ_1 norm solution is slower than the convergence of gradient descent to minimum ℓ_2 norm solution. There is also a small gap between the solution of ℓ_1 regularization and CVXPY. The reason is the regularization coefficient has to be infinitesimal but in practice numerical errors prevent us from training using very small regularization coefficients.

E.4 Visualization of Fourier Adversarial Attacks

In Figs. 8, 10 and 12 we visualize adversarial samples for models available in RobustBench [5]. Fourier- ℓ_∞ adversarial samples are qualitatively different from ℓ_∞ adversarial samples as they concentrate on the object.

Model name	Robust training type
Standard	-
Gowal2020Uncovering_70_16_extra	Linf
Gowal2020Uncovering_28_10_extra	Linf
Wu2020Adversarial_extra	Linf
Carmon2019Unlabeled	Linf
Sehwag2020Hydra	Linf
Gowal2020Uncovering_70_16	Linf
Gowal2020Uncovering_34_20	Linf
Wang2020Improving	Linf
Wu2020Adversarial	Linf
Hendrycks2019Using	Linf
Gowal2020Uncovering_extra	L2
Gowal2020Uncovering	L2
Wu2020Adversarial	L2
Augustin2020Adversarial	L2
Engstrom2019Robustness	L2
Rice2020Overfitting	L2
Rice2020Overfitting	L2
Rony2019Decoupling	L2
Ding2020MMA	L2
Hendrycks2020AugMix_ResNeXt	corruptions
Hendrycks2020AugMix_WRN	corruptions
Kireev2021Effectiveness_RLATAugMixNoJSD	corruptions
Kireev2021Effectiveness_AugMixNoJSD	corruptions
Kireev2021Effectiveness_Gauss50percent	corruptions
Kireev2021Effectiveness_RLAT	corruptions

Table 2: List of models evaluated in Fig. 5.

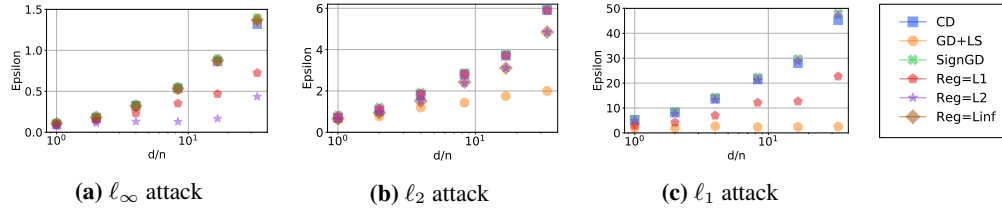


Figure 6: Margin of models in Fig. 2. Models are trained to be robust against ℓ_∞ , ℓ_2 , ℓ_1 attacks. For each attack, there exists one optimizer and one regularization method that finds the maximally robust classifier. Adversarial training also finds the solution given the maximal ε .

F Visualization of Norm-balls

To reach an intuition of the norm-ball for Fourier ℓ_∞ norm, we visualize a number of common norm-balls in 3D in Fig. 14. Norm-balls have been visualized in prior work [81] but we are not aware of any visualization of Fourier- ℓ_∞ .

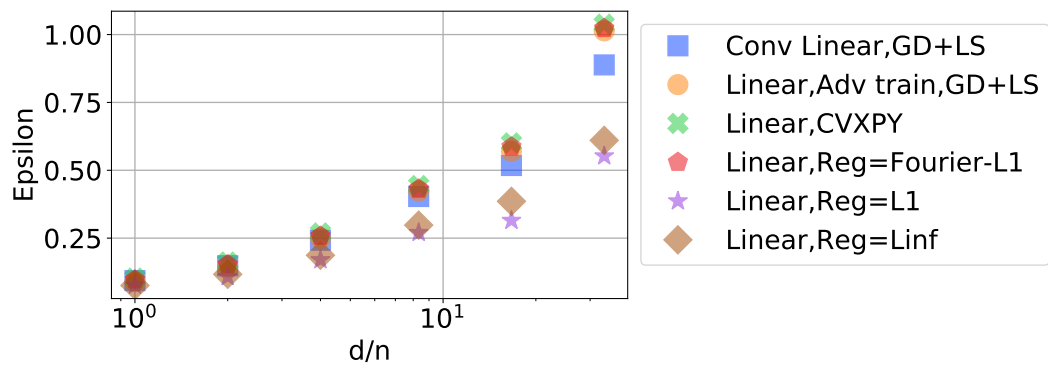


Figure 7: Fourier- ℓ_1 margin of Linear Convolutional Models.

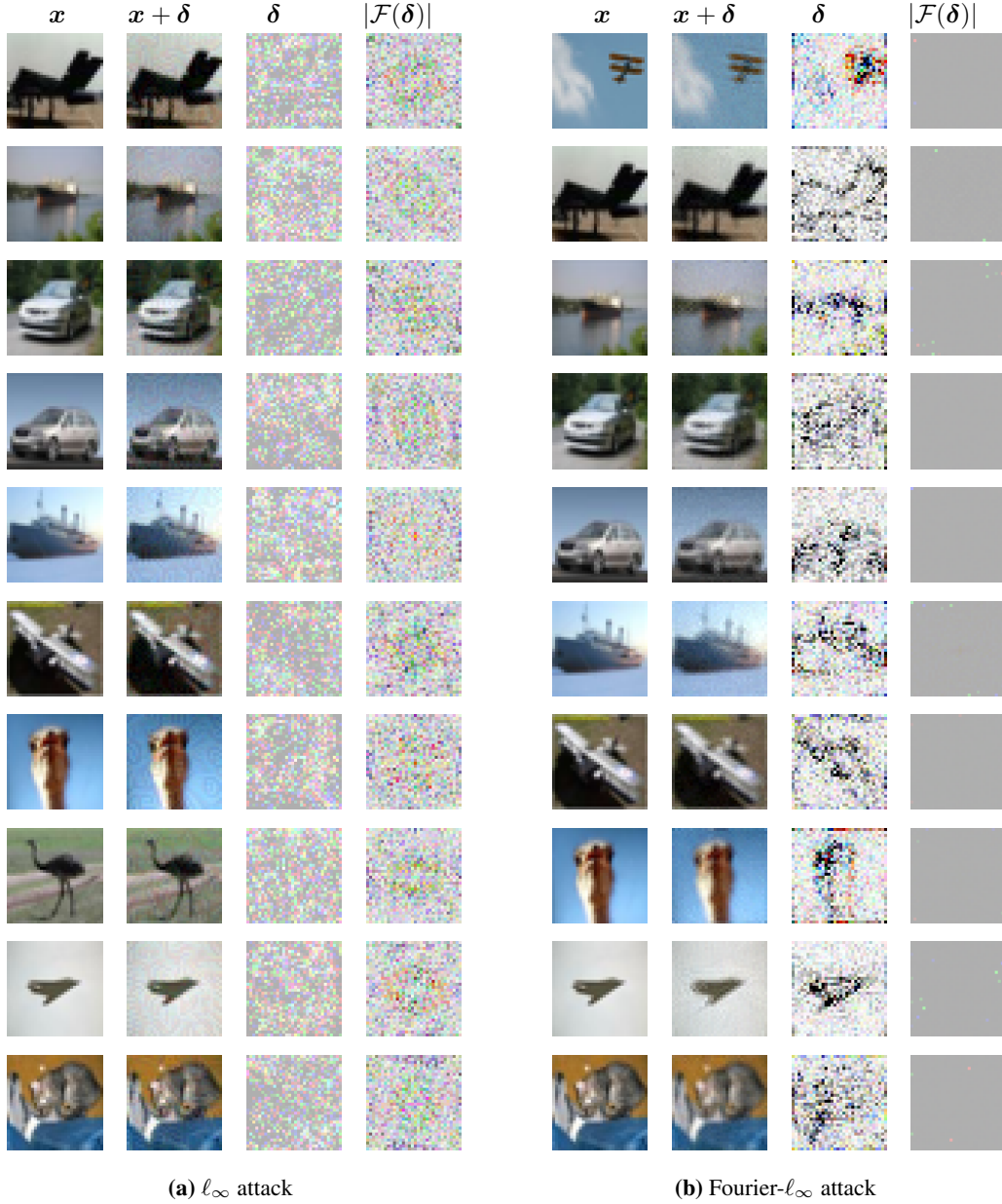


Figure 8: Adversarial attacks (ℓ_∞ and Fourier- ℓ_∞) against CIFAR-10 with standard training. WideResNet-28-10 model with standard training. The attack methods are APGD-CE and APGD-DLR with default hyperparameters in RobustBench. We use $\varepsilon = 8/255$ for both attacks. Fourier- ℓ_∞ perturbations are more concentrated on the object. Darker color in perturbations means larger magnitude. The optimal Fourier attack step is achieved when the magnitude in the Fourier domain is equal to the constraints.

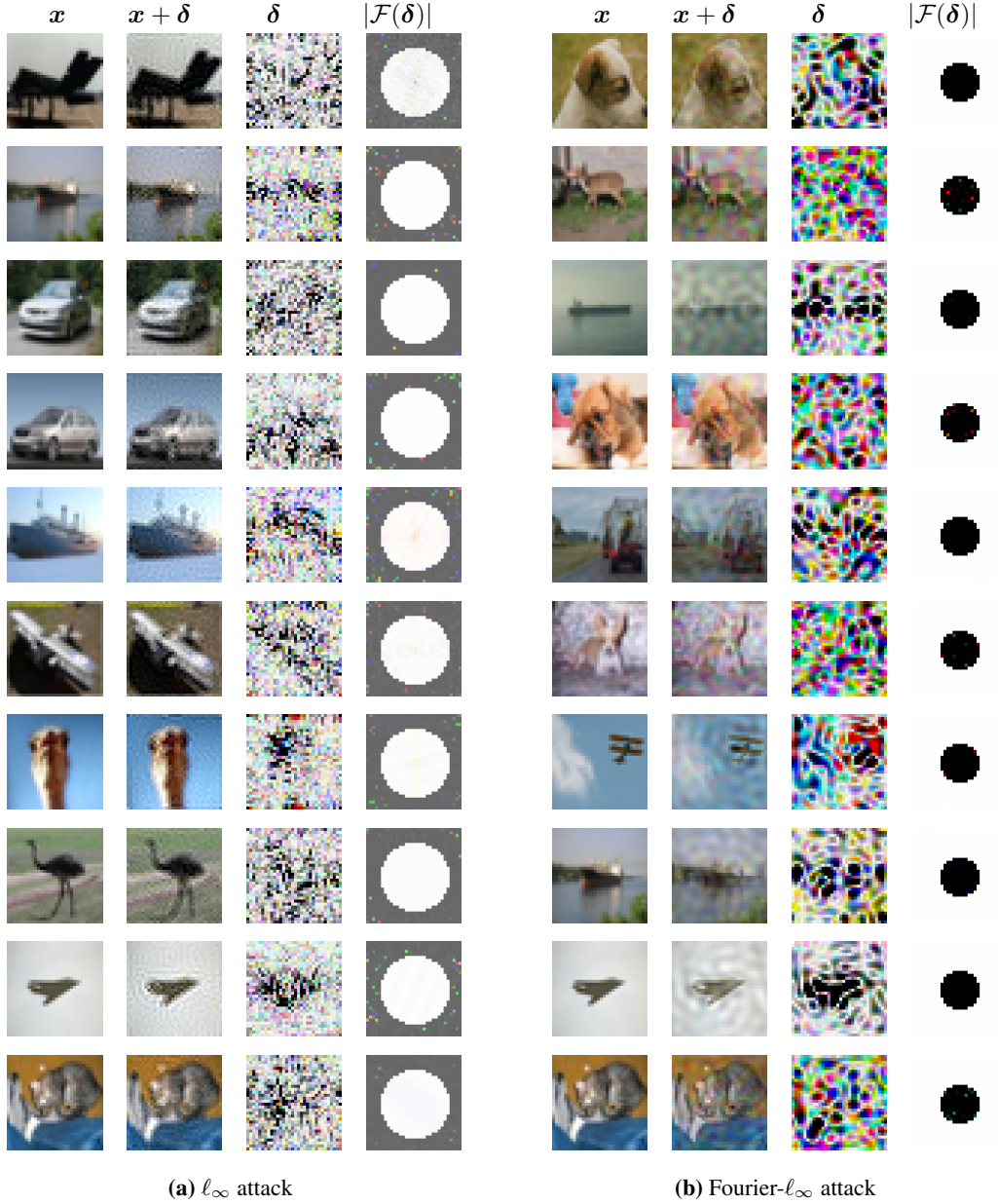


Figure 9: Adversarial attacks (High and low frequency Fourier- ℓ_∞) against CIFAR-10 with standard training. WideResNet-28-10 model with standard training. The attack methods are APGD-CE and APGD-DLR with default hyperparameters in RobustBench. We use $\varepsilon = 15/255, 45/255$ respectively for high and low frequency. Darker color in perturbations means larger magnitude. The optimal Fourier attack step is achieved when the magnitude in the Fourier domain is equal to the constraints.

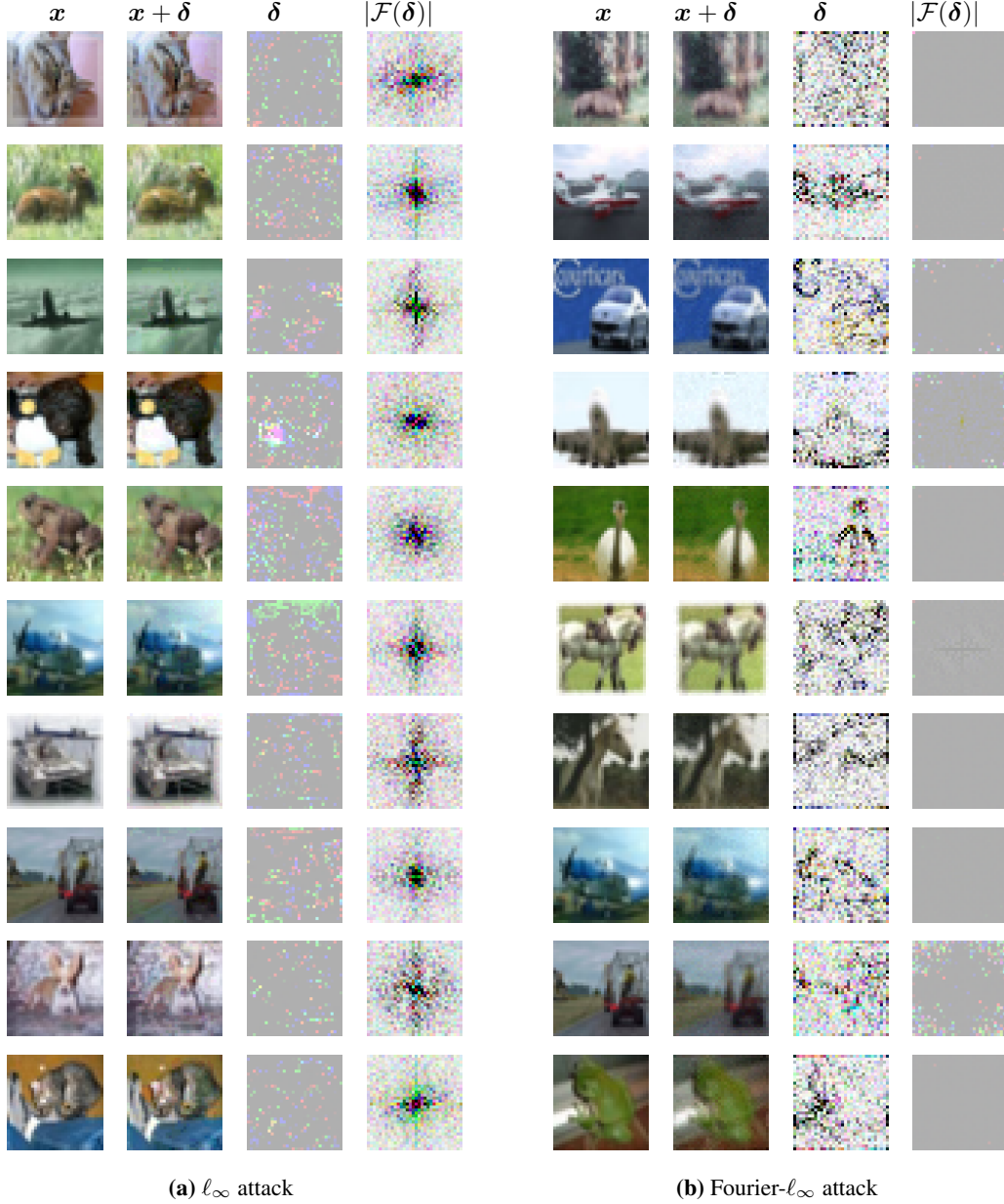


Figure 10: Adversarial attacks (ℓ_∞ and Fourier- ℓ_∞) against CIFAR-10 ℓ_∞ model of [79]. Adversarially trained model against ℓ_∞ attacks. The attack methods are APGD-CE and APGD-DLR with default hyperparameters in RobustBench. We use $\varepsilon = 8/255$ for both attacks. Fourier- ℓ_∞ perturbations are more concentrated on the object. Darker color in perturbations means larger magnitude. The optimal Fourier attack step is achieved when the magnitude in the Fourier domain is equal to the constraints.

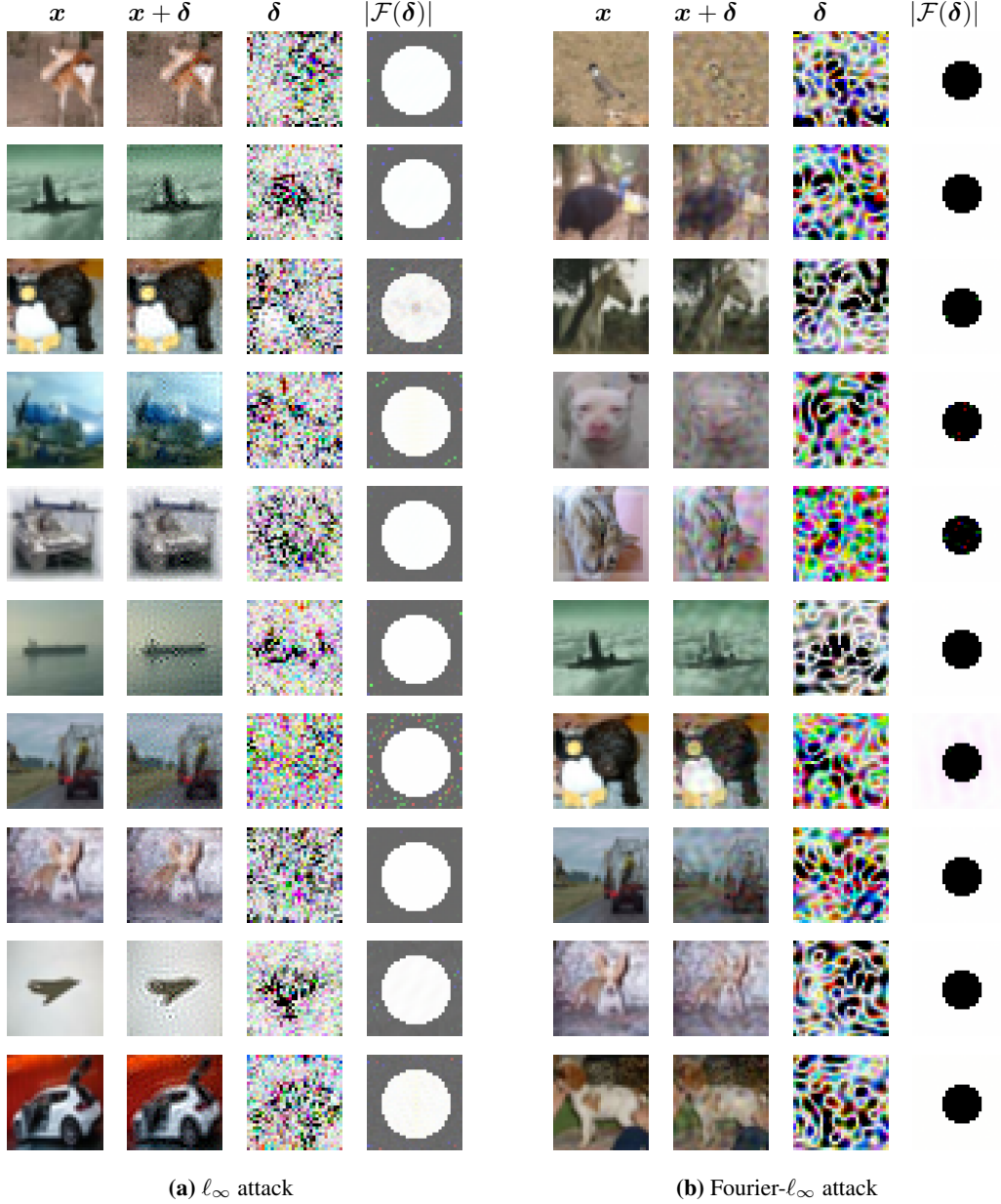


Figure 11: Adversarial attacks (High and low frequency Fourier- ℓ_∞) against CIFAR-10 ℓ_∞ model of [79]. WideResNet-28-10 model with standard training. The attack methods are APGD-CE and APGD-DLR with default hyperparameters in RobustBench. We use $\varepsilon = 15/255, 45/255$ respectively for high and low frequency. Darker color in perturbations means larger magnitude. The optimal Fourier attack step is achieved when the magnitude in the Fourier domain is equal to the constraints.

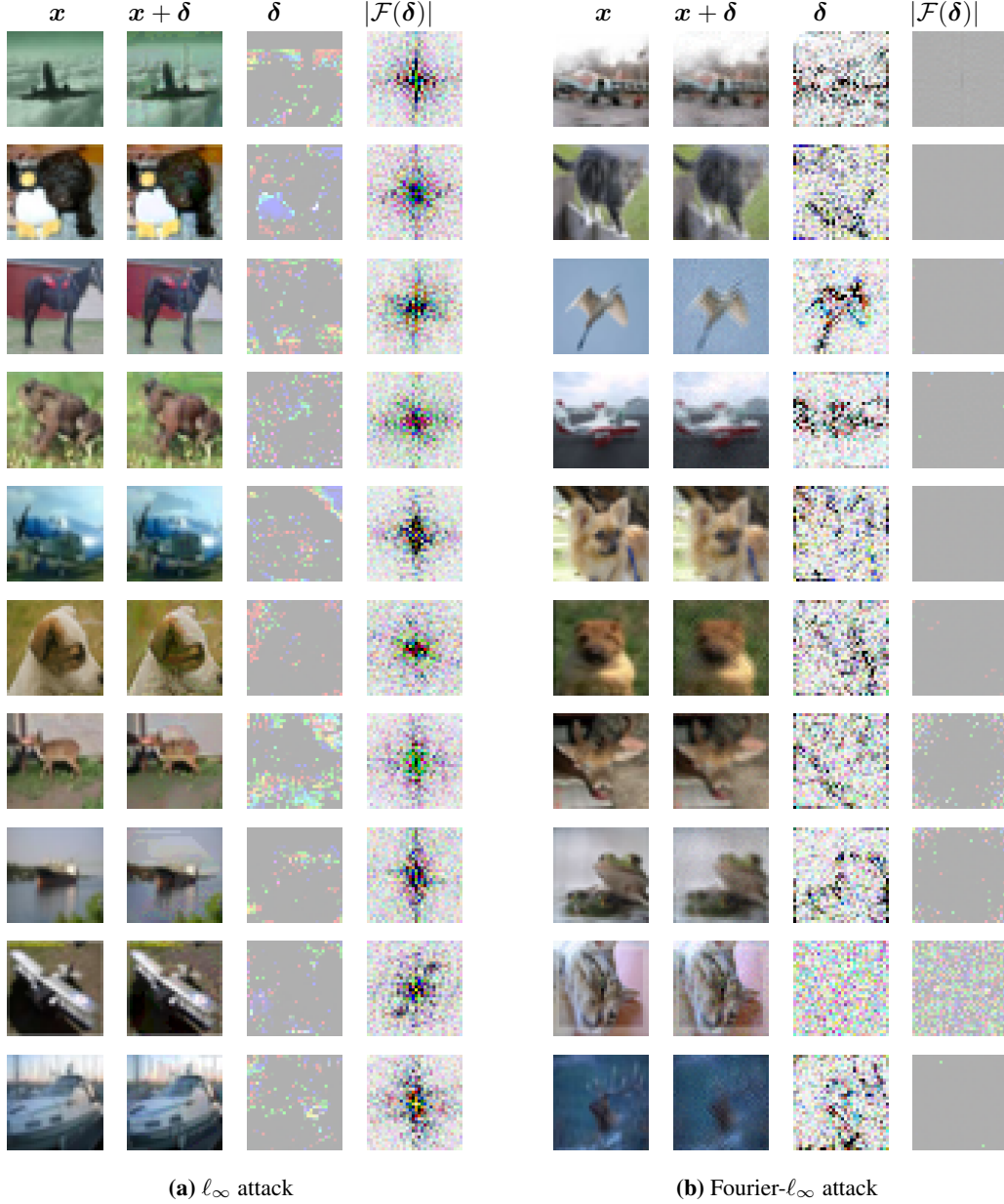


Figure 12: Adversarial attacks (ℓ_∞ and Fourier- ℓ_∞) against CIFAR-10 ℓ_2 model of [80]. Adversarially trained model against ℓ_2 attacks. The attack methods are APGD-CE and APGD-DLR with default hyperparameters in RobustBench. We use $\varepsilon = 8/255$ for both attacks. Fourier- ℓ_∞ perturbations are more concentrated on the object. Darker color in perturbations means larger magnitude. The optimal Fourier attack step is achieved when the magnitude in the Fourier domain is equal to the constraints.

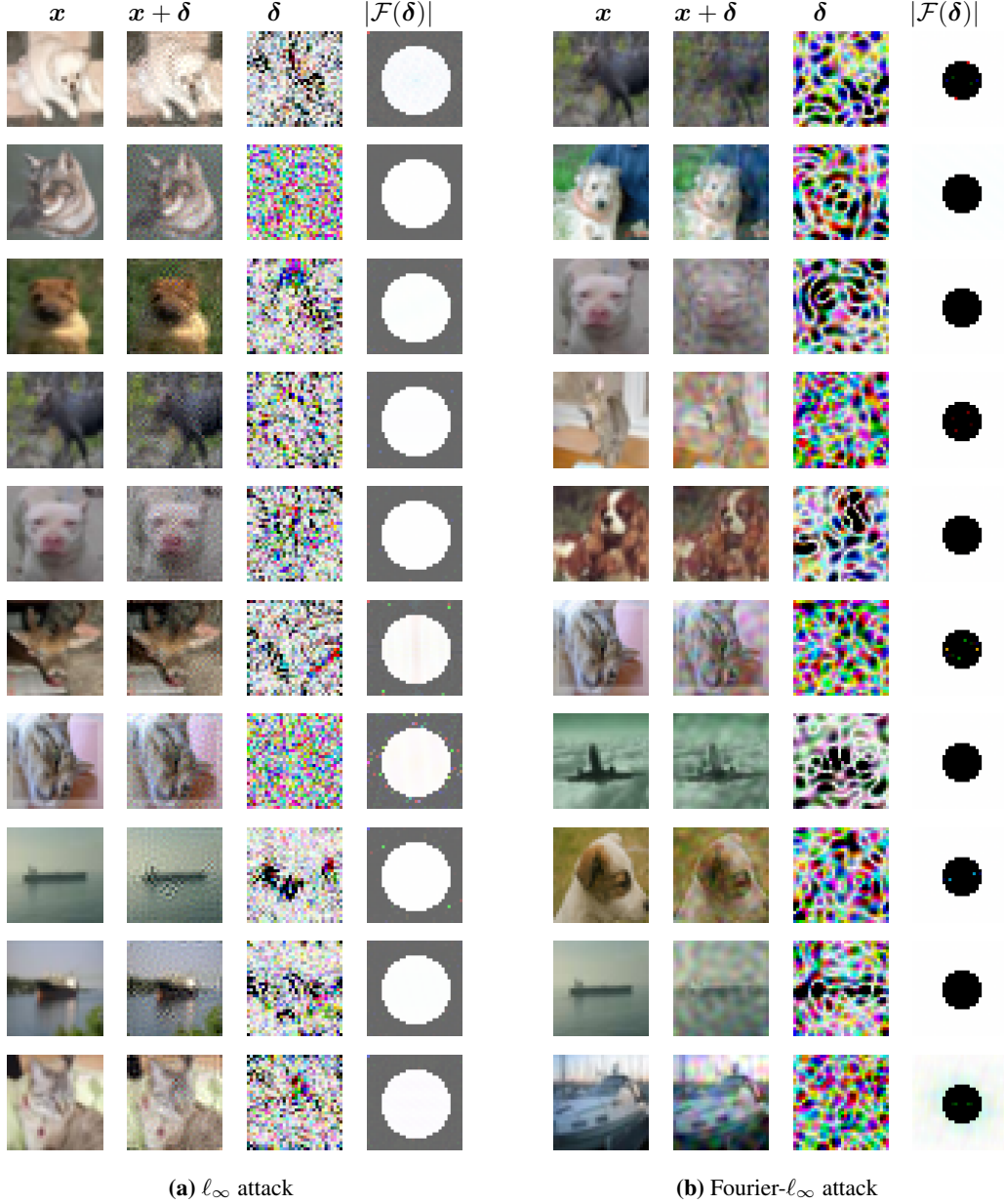
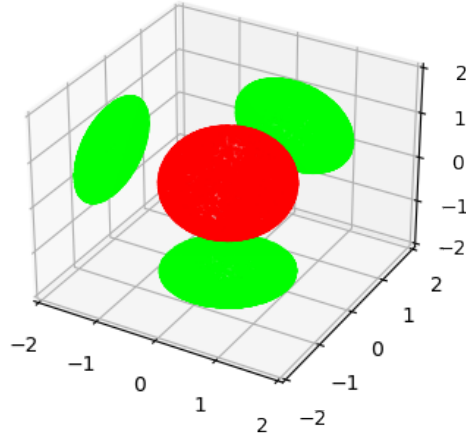
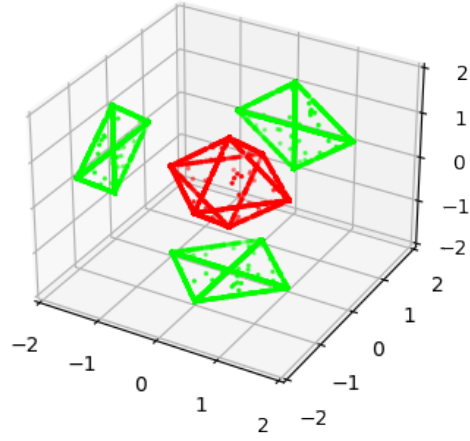


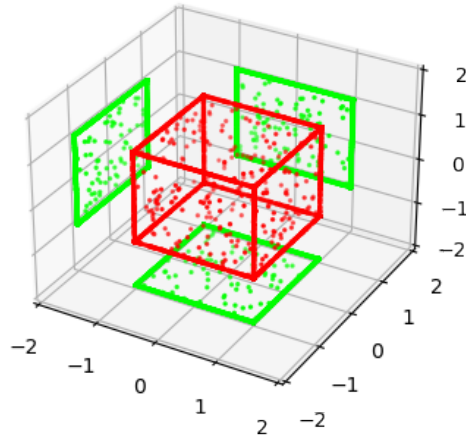
Figure 13: Adversarial attacks (High and low frequency Fourier- ℓ_∞) against CIFAR-10 ℓ_2 model of [80]. WideResNet-28-10 model with standard training. The attack methods are APGD-CE and APGD-DLR with default hyperparameters in RobustBench. We use $\varepsilon = 15/255, 45/255$ respectively for high and low frequency. Darker color in perturbations means larger magnitude. The optimal Fourier attack step is achieved when the magnitude in the Fourier domain is equal to the constraints.



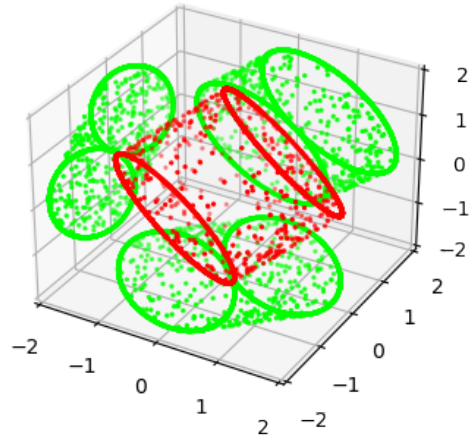
(a) $\|\delta\|_2 = 1$



(b) $\|\delta\|_1 = 1$



(c) $\|\delta\|_\infty = 1$



(d) $\|\mathcal{F}(\delta)\|_\infty = 1$

Figure 14: Unit norm balls in 3-D (red) and their 2-D projections (green). Linear models trained with gradient descent are maximally robust to ℓ_2 perturbations. Two-layer linear convolutional networks trained with gradient descent are maximally robust to perturbations with bounded Fourier- ℓ_∞ .